

MODEL INVESTIGATION OF STRESS DISTRIBUTION
IN THE KNEE OF A SKEWED RIGID-FRAME BRIDGE

by

Michael Charles Cusano

Thesis submitted to the Graduate Faculty of the
Virginia Polytechnic Institute
in candidacy for the degree of

MASTER OF SCIENCE

in

CIVIL ENGINEERING

APPROVED:

APPROVED:

Director of Graduate Studies

Head of Department

Dean of Engineering

Professor in Charge of Thesis

August, 1953

Blacksburg, Virginia

II. TABLE OF CONTENTS

	Page
I. TITLE PAGE	1
II. TABLE OF CONTENTS	2
III. INTRODUCTION	9
IV. REVIEW OF LITERATURE	11
A. Theories of Design	11
B. Full Size Test	16
C. Model Test	18
V. THE INVESTIGATION	21
A. Object of the Investigation	21
B. Method of Procedure	22
C. Method of Testing	28
VI. DATA AND RESULTS	41
VII. DISCUSSION	65
A. Curves	65
B. Interpretation of Curves	67
C. Sidesway	72
VIII. CONCLUSIONS	74
IX. RECOMMENDATIONS	75
X. ACKNOWLEDGMENTS	76
XI. BIBLIOGRAPHY	77
XII. VITA	79

LIST OF FIGURES

	Page
Figure 1. Skewed Arch	12
Figure 2. Detail of Model	24
Figure 3. Photograph of Model and Base	25
Figure 4. Detail of Fillet Weld	29
Figure 5. Abutment Base	29
Figure 6. Base Frame	29
Figure 7. Loading Devices	32
Figure 8. Photograph of Concentrated Load Test Apparatus	33
Figure 9. Photograph of Uniform Load Test Apparatus	35
Figure 10. Sample Calculation Sheet	44
Figure 11. Stress Distribution-Uniform Load Section AA	45
Figure 12. Stress Distribution-Uniform Load Section BB	46
Figure 13. Stress Distribution-Concentrated Load Panel O Section AA	47
Figure 14. Stress Distribution-Concentrated Load Panel O Section BB	48
Figure 15. Stress Distribution-Concentrated Load Panel I Section AA	49
Figure 16. Stress Distribution-Concentrated Load Panel I Section BB	50
Figure 17. Stress Distribution-Concentrated Load Panel II Section AA	51

	Page
Figure 18. Stress Distribution-Concentrated Load Panel II Section BB	52
Figure 19. Stress Distribution-Concentrated Load Panel III Section AA	53
Figure 20. Stress Distribution-Concentrated Load Panel III Section BB	54
Figure 21. Stress Distribution-Concentrated Load Panel IV Section AA	55
Figure 22. Stress Distribution-Concentrated Load Panel IV Section BB	56
Figure 23. Stress Distribution-Concentrated Load Panel V Section AA	57
Figure 24. Stress Distribution-Concentrated Load Panel V Section BB	58
Figure 25. Stress Distribution-Concentrated Load Panel VI Section AA	59
Figure 26. Stress Distribution-Concentrated Load Panel VI Section BB	60
Figure 27. Stress Distribution-Concentrated Load Panel VII Section AA	61
Figure 28. Stress Distribution-Concentrated Load Panel VII Section BB	62
Figure 29. Stress Distribution-Concentrated Load Panel VIII Section AA	63
Figure 30. Stress Distribution-Concentrated Load Panel VIII Section BB	64
Figure 31. Linear Stress Distribution	67
Figure 32. Deflection at Corners of the Deck	73

LIST OF TABLES

	Page
Table 1. Physical Properties of Aluminum	27
Table 2. Per Cent Difference of Applied Load and Thrust	69
Table 3. Stress Concentration Factors	71

LIST OF SYMBOLS

<u>Symbol</u>	<u>Definition</u>
1. <u>Symbols used on figures</u>	
C	A point on the neutral surface of the arch
T	Internal force acting at C
M	Internal moment acting at C
v	Axis through C, tangent to the neutral surface, perpendicular to the abutments
u	Axis through C, perpendicular to v axis and arch surface
z	Axis through C, perpendicular to u and v axes
T_u, T_v, T_z	Components of T along u, v, and z axes
M_u, M_v, M_z	Components of M about u, v, and z axes
X	Horizontal axis perpendicular to abutments and intersecting the base of the abutment at mid-point
Z	Vertical axis perpendicular to the X axis, and hinge line, at the mid-point of the base of the abutment
Y	Axis perpendicular to X and Z axes at their point of intersection
R_x, R_y, R_z	Components of the total reaction at the base of the abutment along X, Y, and Z axes
M_x, M_y, M_z	Components of total moment at base of abutment about X, Y, and Z axes

2. Symbols used in experimental work

E	Modulus of elasticity
ν	Poisson's ratio
ϵ	Unit strain
σ	Unit stress
$\epsilon_x, \epsilon_y, \epsilon_z$	Unit strain in direction of X, Y, and Z axes
$\sigma_x, \sigma_y, \sigma_z$	Unit stress in direction of X, Y, and Z axes
$\epsilon_x)_t, \epsilon_y)_t$	Unit strain on top surface of deck in direction of X and Y axes
$\epsilon_x)_b, \epsilon_y)_b$	Unit strain on bottom surface of deck in direction of X and Y axes
$\epsilon_z)_i, \epsilon_y)_i$	Unit strain on inside face of abutment in direction of Z and Y axes
$\epsilon_z)_o, \epsilon_y)_o$	Unit strain on outside face of abutment in direction of Z and Y axes
$\sigma_x)_t$	Unit stress on top surface of deck in direction of X axis
$\sigma_x)_b$	Unit stress on bottom surface of deck in direction of X axis
$\sigma_z)_i$	Unit stress on inside face of abutment in direction of Z axis
$\sigma_z)_o$	Unit stress on outside face of abutment in direction of Z axis
$\sigma_z)_i'$	Unit stress on inside face of abutment in direction of Z axis obtained from symmetry of model
$\sigma_z)_o'$	Unit stress on outside face of abutment in direction of Z axis obtained from symmetry of model

V Thrust in abutment
 ΣV Sum of thrust in both abutments
K Stress concentration factor
t Thickness of plate
W Applied load

III. INTRODUCTION

The increase in the speed of the automobile and the increase in the volume of traffic has presented many problems to the highway designer, one of the most important being the elimination of grade crossings.

The rigid frame bridge, introduced in this country in the early 1920's, offered a very satisfactory solution to the problem of grade separation. This type of structure was used quite extensively by the Westchester County Park Commission in the expansion of the highway system of lower New York State. The rigid frame is more economical, has greater simplicity, and is more adaptable to architectural treatment than the more conventional deck or through girder bridge.

The problem of grade separation was simplified to a still greater degree by the use of the skewed rigid frame, but due to the complexity of analyzing this type of structure it's use was limited in early installations.

Early theories for the analysis of the skewed type of structure were based on the theories of the right rigid frame and arch, but when these theories proved inadequate it was necessary to develop a more rigorous analysis. Although the new theories were accurate, they were also much too involved

for practical use and certain assumptions were made to reduce their complexity.

Although the newly developed theories did solve the problem of analyzing the skewed rigid frame, another problem arose, namely that of the validity of the assumptions. Although structural failures were few, the use of high, and in some respects indeterminate, factors of safety may well have compensated for any errors in the assumptions.

Committee 314 of the A.C.I. is now making a study of the rigid frame bridge. It is hoped that at some time in the near future a theory, more in keeping with the true behavior of the skewed rigid frame, will be developed.

The Committee has decided that model tests offer a convenient solution to many of the problems arising in the development of a new theory.

It is the purpose of this thesis to find the stress distribution at the knee of a skewed rigid frame bridge model for various loading conditions.

IV. REVIEW OF LITERATURE

A. Theories of Design

The practicability of the skewed structure as a means of grade separation or for bridging obstructions, obviously occurred to the bridge designer long before the skewed structure was used. The factor which delayed it's use was the complexity of the analysis of this type of structure.

Theories proposed for the right rigid frame were not applicable to the skewed structure since they did not consider the additional force arising due to the skewed slab. It was thus necessary to develop a definite theory which would apply to the skewed rigid frame.

1. Theory of J. C. Rathbun. (7,8)

In 1924, J. C. Rathbun presented a theory for the analysis of stress in skewed arches. Although this theory was developed for skewed arches originally, it was also applicable to the skewed rigid frame.

Rathbun divided the arch into two cantilever segments by passing a plane through the arch perpendicular to the free edges and parallel to the axis of the barrel, as shown in Figure 1. This resulted in a curved cantilever beam, rigidly fixed at the abutments and subjected to the loads, and the

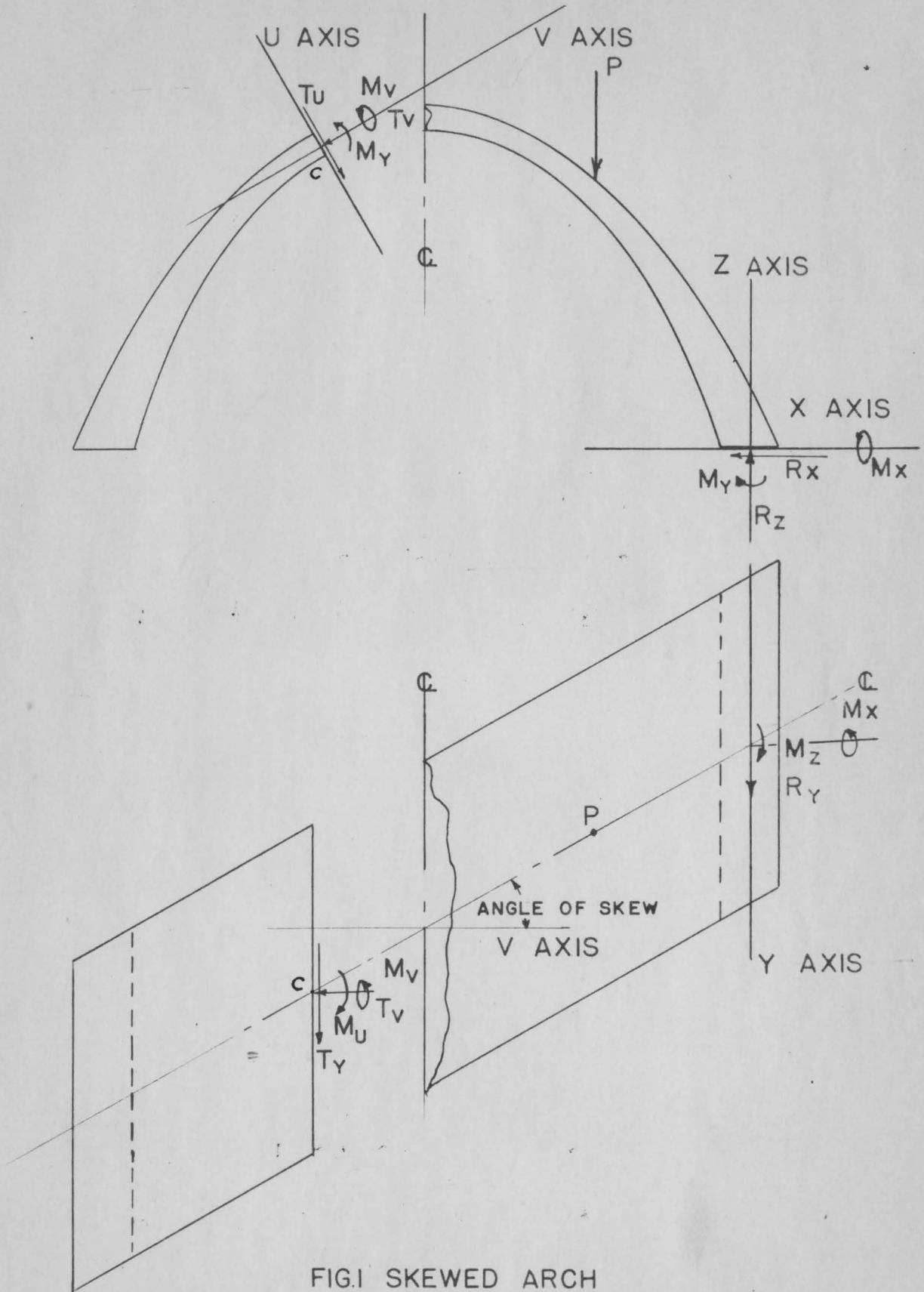


FIG.1 SKEWED ARCH

the force and moment developed by the other half of the arch at the plane of intersection of the two halves. The problem thus reduced itself to one of finding what forces and moments were necessary to keep the two curved beams coincident, at their plane of intersection, when movement, due to the application of external loads, occurred.

Writing one elastic equation for each of the redundant reactions, Rathbun developed six equations with six unknowns, which had to be solved simultaneously for the unknown quantities T_u , T_v , Y_y , M_u , M_v , and M_y . Both the number of equations and the number of unknowns reduced to five when the assumption was made that T_u was equal to zero.

2. The Method of A. G. Hayden.⁽⁴⁾

At the request of A. G. Hayden, Design Engineer with the Westchester County Park Commission, Rathbun, in 1927, extended his theory to include symmetrical structures, hinged at the supports. The analysis was not published as such, but a description may be found in a book written by Hayden entitled, "The Rigid Frame Bridge".

This method was not as complex as Rathbun's original theory since it was concluded that the total vertical reactions were the same as those that occurred in a simple

beam of the same span with a width equal to the skew width of the arch.

3. Design Method of B. L. Weiner. (9)

In 1932, Bernard L. Weiner, in an attempt to simplify the theory of Rathbun, presented a simplified method of design. In his paper, Weiner develops a theory for the distribution of stresses produced for various forces and couples acting on a section of the skew frame. A method is also discussed for the determination of the maximum stresses.

4. The Simplified Method of R. M. Hodges. (5)

In an attempt to present a theory for skewed reinforced concrete frames and arches, which was free of the evident inconsistency of the assumptions regarding the rotation of the footings of skewed frames and arches, Richard M. Hodges presented a paper entitled, "Simplified Analysis of Skewed Reinforced Concrete Frames and Arches", in 1944. The analysis was based on the assumption, ordinarily made of the action of soil foundations in the analysis of rigid frame bridges, that a virtual hinge exists along the Y axis at the base of the footing due to the compressibility of the soil. Assuming that the reactions R_x at the base of the abutment normal to the face of the abutment, were the same as those that

occurred in a right rigid frame, Hodges developed a simplified theory.

The identity used by Hodges was proposed nine years before by Edward P. Gifford.

5. Methods of M. Barron⁽¹⁾ and B. L. Weiner.⁽¹⁰⁾

In 1950, both Maurice Barron and Bernard L. Weiner proposed simplified theories of analysis for the skewed rigid frame bridge. These theories presented a method by which the resisting forces and moments in the hinge are first computed for a rectangular rigid frame, and the effects of the skewed structure are then determined separately. The method reduces to a comparison of the skewed frame and the right frame.

6. Method of J. P. Michalos.⁽⁶⁾

A numerical method was proposed, for the analysis of single span rigid frames and arches, by James P. Michalos in 1952. The method may be applied to structures which are non-symmetrical, are hinged or fixed at the supports, and subjected to loads or deformations from any direction.

B. Full Size Tests

In an attempt to check the theories of design in use, some tests have been made on existing structures. Unfortunately, the number of tests have been few and only a very small number are discussed in the literature. Those appearing in the literature are described below.

1. Central Avenue Bridge, Glendale, California. (12,13)

The Central Avenue Bridge at Glendale, California, was made available for test purposes in 1936. The bridge was designed by the Hayden method and had a solid deck, with a span, perpendicular to the abutments, of 43 feet, width along abutments of 60 feet, and a skew angle of 26 degrees. At the time it was made available for the tests the structure was two years old.

Loading was accomplished by use of 3000 lb. steel ingots spread at various distances along the transverse centerline in a 3 ft. wide strip. By attaching 10 in. Whittemore and 2 in. Berry strain gages to the exposed reinforcing rods, strains were measured at the haunch and crown. Deflections of the crown, deck corners, and bottom of the abutments were measured by dial gages.

The published results⁽¹³⁾ contained only a few conclusions. From the available data it was apparent that:

- (a) tension steel at the obtuse corners had the highest stress, but over the entire deck the unit stress never exceeded 10,000 psi,
- (b) a rotation of the entire structure was noted, and
- (c) maximum deflections at the crown, under the greatest load (440 tons), was approximately $3/8$ in.

After the completion of the test the structure was wrecked by the Army Engineers.

The high safety factor encountered was most significant. The maximum applied load, concentrated along the centerline, was about four times larger than the maximum safe design load.

2. North Avenue Bridge, Chicago, Illinois.⁽¹⁴⁾

Upon the completion of the North Avenue Bridge in 1940, a check was made on certain assumptions made in it's design. This bridge was a skewed, two hinged, reinforced concrete rigid frame of slab and girder design with hinges tied by reinforcement of the lower roadway slab. The deck span was 101 ft., width along abutments 130 ft., and skew angle 55 degrees.

During construction, special extensometer stations were built into the deck girders, tie slab, and abutments. Strain measurements were taken due to the action of the dead load, uniform load along the crown, and uniform longitudinal load on the centerline of the middle girder. The temperature variation over a period of four months and its effect on hinge movements and deck deflections were recorded.

The results of this test indicated that for the particular loads applied, the behavior of the structure was similar to the assumed action, i.e., torsional effects were negligible for this T-beam type deck.

C. Model Tests

1. Model Investigations of Edward F. Gifford. (11)

The literature revealed that model tests on a skewed rigid frame were conducted by E. F. Gifford in 1932. The models used in Gifford's tests had a skew angle of 45 degrees and were constructed of concrete and square mesh, #14 wire, with a prototype to model scale of 64.

Concentrated loads were applied at the center and quarter points and the models tested to destruction. Only the appearance and description of cracks were noted.

The first cracks in each case appeared at the obtuse corners and continued approximately perpendicular to the direction of traffic.

2. Investigations of G. P. Fisher and W. G. Boyer. (2)

Gordon P. Fisher and Walter C. Boyer conducted a series of tests on a model of a two-span, rigid frame, skewed bridge in order to determine the reactions.

The basic structure studied was a hinged, two-span rigid frame of two equal square spans 100 ft. long with a central pier of 22 ft., which was satisfactory for model analysis when scaled down. Effect of skew on the reactions was investigated for skew angle variation from 0 to 50 degrees, in increments of 10 degrees. The deck was flat, constant in thickness, and 40 ft. wide.

The investigation was based on the deformer method as developed by Beggs and modified by William J. Eney. Influence lines were obtained by use of controlled deflections rather than applied loads.

The authors arrived at the following conclusions:

- (a) the vertical reactions and horizontal thrusts are essentially independent of the skew for centerline loading. (There is some effect for off center loading.)
- (b) the

horizontal-plane moments, M_z , proved to be negligible, (c) a serious discrepancy between experiment and theory was found for the torsional moments, M_x , at the base of the abutment, and (d) experimental off-center values for the torsional moment, M_y , about an axis perpendicular to the deck, were completely at variance with the theoretical values and indicated a basically different type of slab action.

The results were compared with Rathbun's theory and the discrepancies were attributed to the use of the torsional factor F.

V. THE INVESTIGATION

A. Object of the Investigation

As stated previously, in order to make the theories developed for skewed rigid frame bridges of practical value to the designing engineer, certain assumptions had to be made. The scarcity of test data to check the assumptions leaves room for doubt concerning the validity of these assumptions. The use of high and, in some respects indeterminate safety factors, leads to highly over-designed structures. These high factors of safety may well compensate for any erroneous assumptions.

Field tests on existing structures are often inconvenient and expensive. It is possible though, through the use of models and instruments such as SR-4 strain gages and Ames dials, to obtain data which would be in agreement with data obtained from tests on the prototype of the model.

It is the purpose of this thesis to obtain the stress distribution that occurs in the knee of a skewed rigid frame bridge under certain loading conditions. These distributions will be obtained by using an aluminum model and SR-4 strain gages.

B. Method of Procedure

1. Model.

It was decided to use a model which would be subject to the laws of the theory of elasticity. For this to be true, the material used in the construction of the model had to be homogeneous and isotropic. Although this is not the actual case for bridges constructed of concrete, the concrete is assumed to exhibit these properties when the design is based on the elastic theory. It was decided to construct the model of aluminum.

Several types of construction were attempted before a satisfactory model was attained.* The first attempt was unsuccessful due to the use of material which was too thin and the inability of obtaining strain measurements large enough to be measured accurately. It was then decided to cast a model of aluminum with a thickness four times that of the first model. Poor casting resulted in a failure under a small central loading.

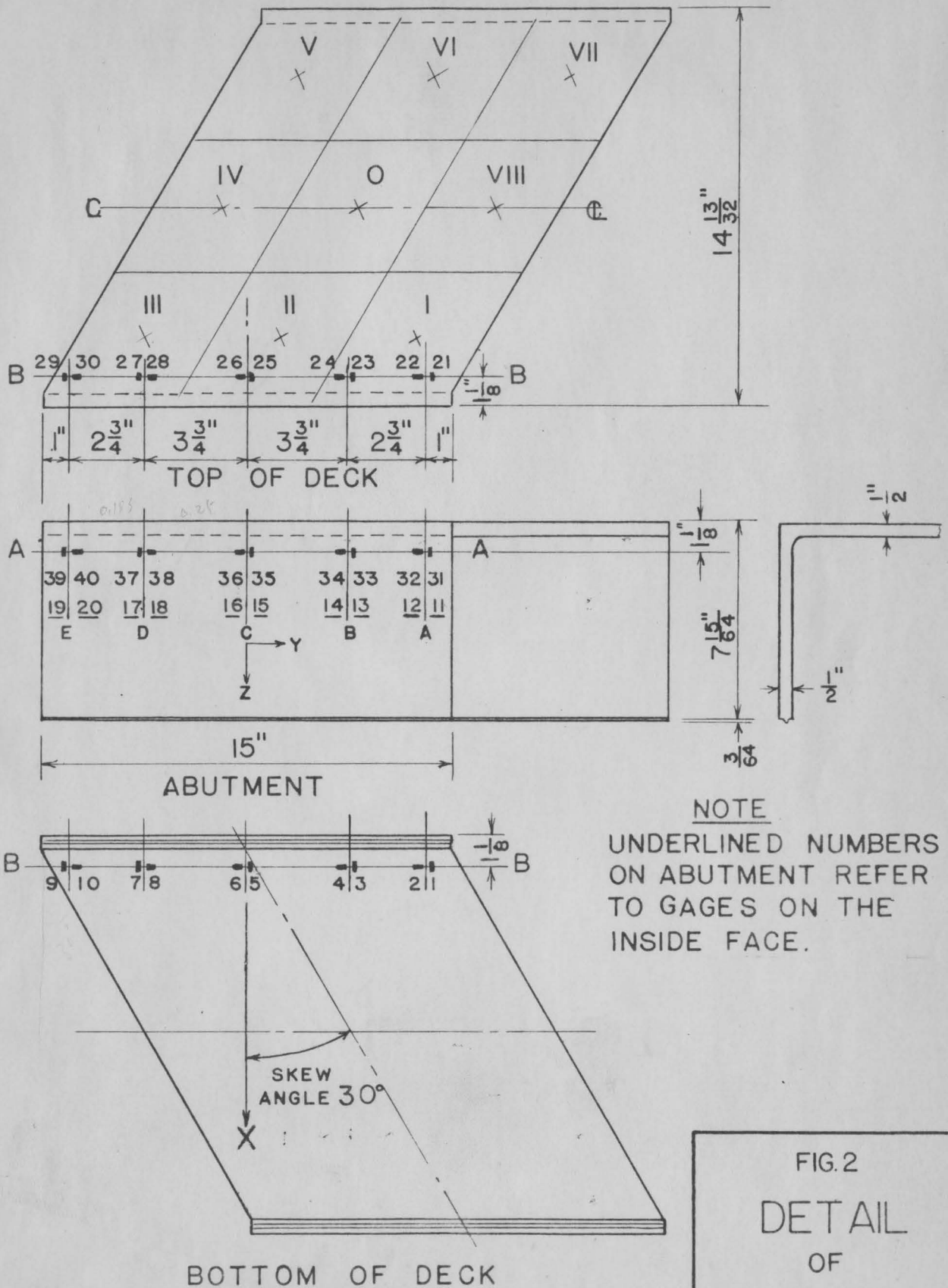
* Data on construction of model and testing of physical properties of aluminum were obtained from "Progress Report on Rigid Frame Bridges", prepared by D. H. Pletta, Chairman, AIC Committee 314, Jan. 15, 1953.

The third attempt at construction of a suitable model proved successful. The model was fabricated by The Aluminum Company of America from 1/2 inch rolled 24S plate, welded along the knee. Welding was accomplished with a ... "semi-automatic inert gas metal arc using 1/16 inch diameter, 43S filler wire, 250 amps D.C. and 50 cubic feet/hour of argon gas flow. A vee-joint was used and filled with two passes on the outside and one on the inside to provide the fillet".* The angle of skew was 30 degrees.

Precautions were taken to prevent warping. Although some warping did occur it was not severe enough to warrant rejection of the model. To relieve thermal stresses, due to welding ... "the model was heat treated to T4, following the welding, by heating to 920°F, holding for one hour, and water quenching".*

The final machining of the model was done at V. P. I. A key was provided at the base of the abutments so that a hinged base could be realized, Figure 5.

The physical properties of the aluminum were tested at V. P. I. according to A. S. T. M. standards.



NOTE
UNDERLINED NUMBERS
ON ABUTMENT REFER
TO GAGES ON THE
INSIDE FACE.

FIG. 2
DETAIL
OF
MODEL



Fig. 3 Model and Base

The aluminum for the test specimens was obtained from the excess metal cut from the model during its final machining. Two specimens were taken parallel and two perpendicular to the direction of rolling of the original plate. The properties are listed in Table 1.

From the similarity of the results, the assumptions regarding the isotropic nature of the model material are justified.

2. SR-4 Strain Gages.

The strains along sections AA and BB of the abutments and deck, respectively, were measured by means of SR-4, type A-7 strain gages with a resistance of 120 ohms. The surface of the bridge where the gages were to be attached was made smooth by rubbing with a fine grade emery cloth, and cleaned with a solvent to remove any substance which might interfere with the action of the strain gages. The gages were attached to the models at the points shown in Figure 2, with Duco #5458 cement. After allowing for sufficient time for the gages to adhere to the bridge, the lead wires were soldered to the gages. All gages at the knee were soldered to a common ground wire which consisted of a bared length of copper wire insulated from the bridge by small blocks of wood and friction

Table 1
Physical Properties of Aluminum

Specimen #	Direction of Rolling	Prop. Limit psi	Ult. Strength psi	Modulus of Elasticity (psi)		% Elong.	Poisson's Ratio
				Dial Ext.	SR-4 Gages		
1	Parallel	32,300	68,750	10,100,000	--	22.0	--
2	Parallel	32,400	68,600	10,450,000	10,950,000	19.5	0.321
3	Perpendicular	29,650	66,800	10,460,000	--	12.5*	--
4	Perpendicular	31,600	66,900	10,460,000	10,920,000	20.0	0.319

* Failure outside gage marks.

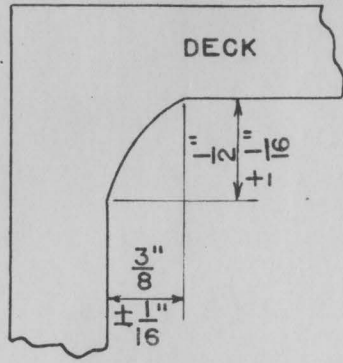
tape, on the abutment. Lead wires from the active legs of the strain gages were fastened to the bridge with Duco cement and gripped together with strips of friction tape. This method was followed in order to protect the gages from accidental damage due to movement of the lead wires. The method worked very well.

To protect the gages during the uniform load test it was necessary to cover the gages with Armstrong A-2 cement. This prevented the gages from being damaged due to the stretching of the rubber during the uniform load test. Preparatory to covering the gages, the lead wires from the gage leads were insulated from the bridge by placing a strip of masking tape under the leads. The cement was then placed over the gages and the lead wires. Tests conducted to determine the effect of Armstrong A-2 cement on the reading of the gages were negative.

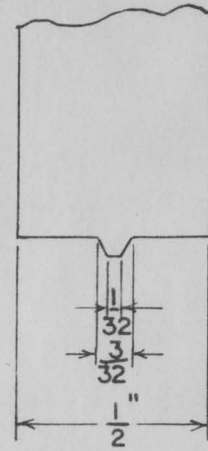
C. Method of Testing

1. Base.

In order to insure positive seating of the model it was necessary to construct a base into which the model could be set and leveled. A detail of the base is shown in Figure 6. The base was constructed of 1" x 3/8" steel bars, fastened



DETAIL
OF
FILLET WELD
FIG. 4



ABUTMENT BASE
FIG. 5

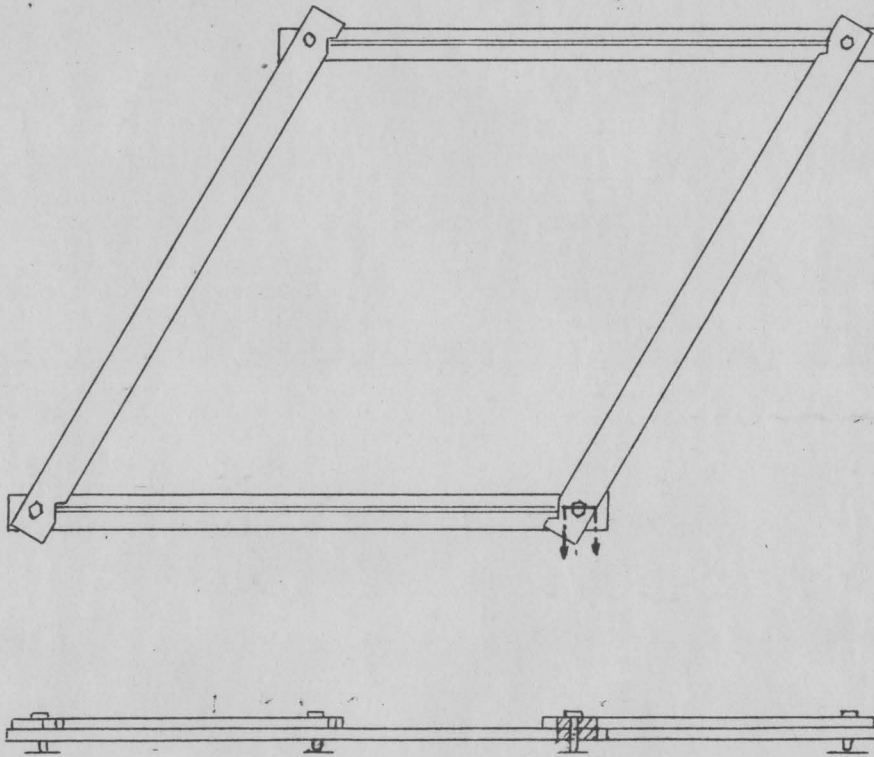


FIG. 6 BASE FRAME

together by bolts. The steel bars into which the abutment fitted had a groove milled into them to match the key which was provided on the bottom of the abutment. The two bars under the abutment were tapped to accommodate the bolts used to fasten the frame together. This made it possible to level the model in the testing machine.

After the model was placed in the frame and leveled, it was removed from the testing machine. To provide a firm base for the model it was necessary to set the base frame in Plaster of Paris. Waxpaper was placed on the table of the testing machine and Plaster of Paris placed on it after which the model and base were placed in the plaster, making sure that the model was properly seated in the base. To insure a good setting of the model and base frame in the plaster, a load of 200 lbs. was placed on the model with the testing machine for a length of time necessary for the plaster to set.

Inspection of the base after the plaster had set insured that a firm base was attained.

2. Method of Loading.

All tests were performed with a 60,000 pound capacity Tinius Olsen Universal testing machine, using the 6,000 pound testing range.

a. Concentrated load test. The model was investigated for the stress distribution in the knee due to concentrated loads at various points on the deck and for a uniform load on the complete surface of the deck.

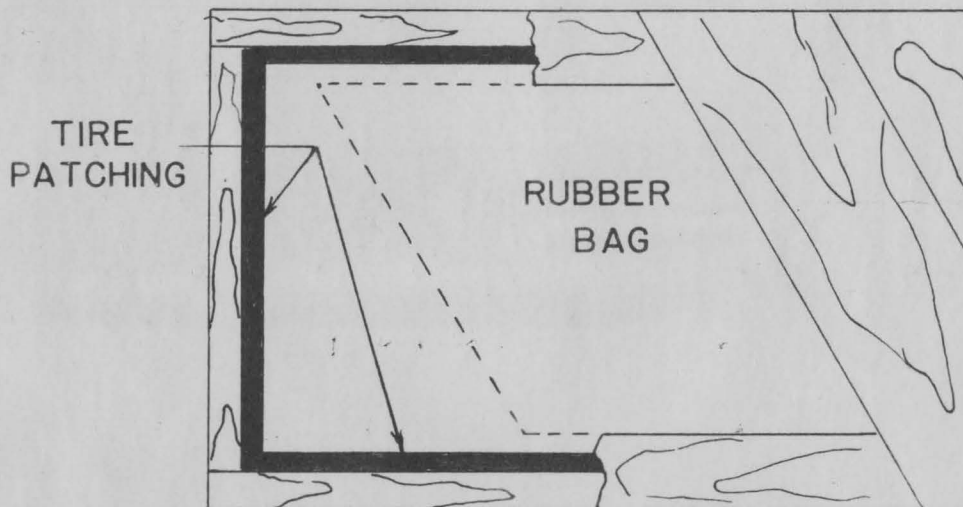
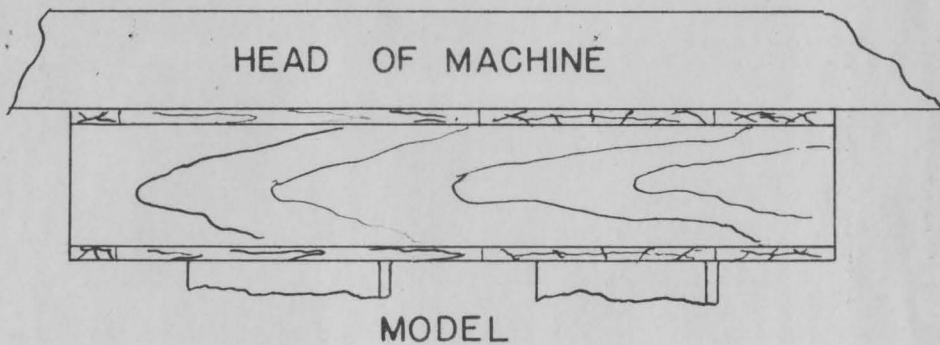
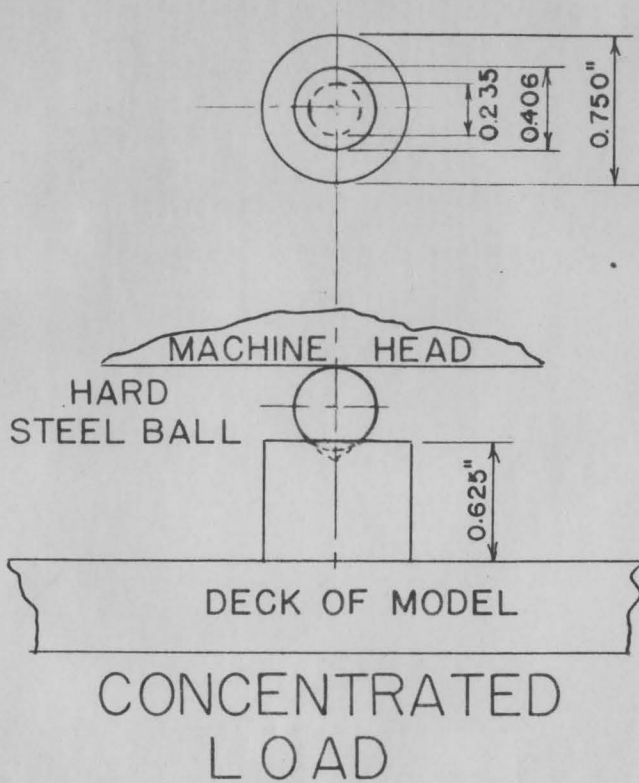
The surface of the deck was divided into nine panels by marking equi-spaced lines parallel to the edges of the deck. The panels were numbered as shown in the detail of the model in Figure 2. The point of application of the load was determined by the intersection of the diagonals of the panel.

The concentrated load was applied by means of a $3/4"$ ϕ x $5/8"$ cylinder and a $0.406"$ diameter hard steel ball as shown in Figure 5. The cylinder was used to obtain a ring loading and thus eliminate the deleterious effects of a concentrated load.

The load was applied through the machine head moving at the rate of 0.035 to 0.05 inches per minute.

The method of loading proved to be satisfactory as an inspection of the surface of the bridge gave no indication of indentation.

b. Uniform load test. Application of the uniform load test to the model presented a slight problem. From the results of the concentrated load test it was realized that a total vertical load of at least 1500 pounds would have to be



UNIFORM LOAD

FIG. 7 LOADING DEVICES

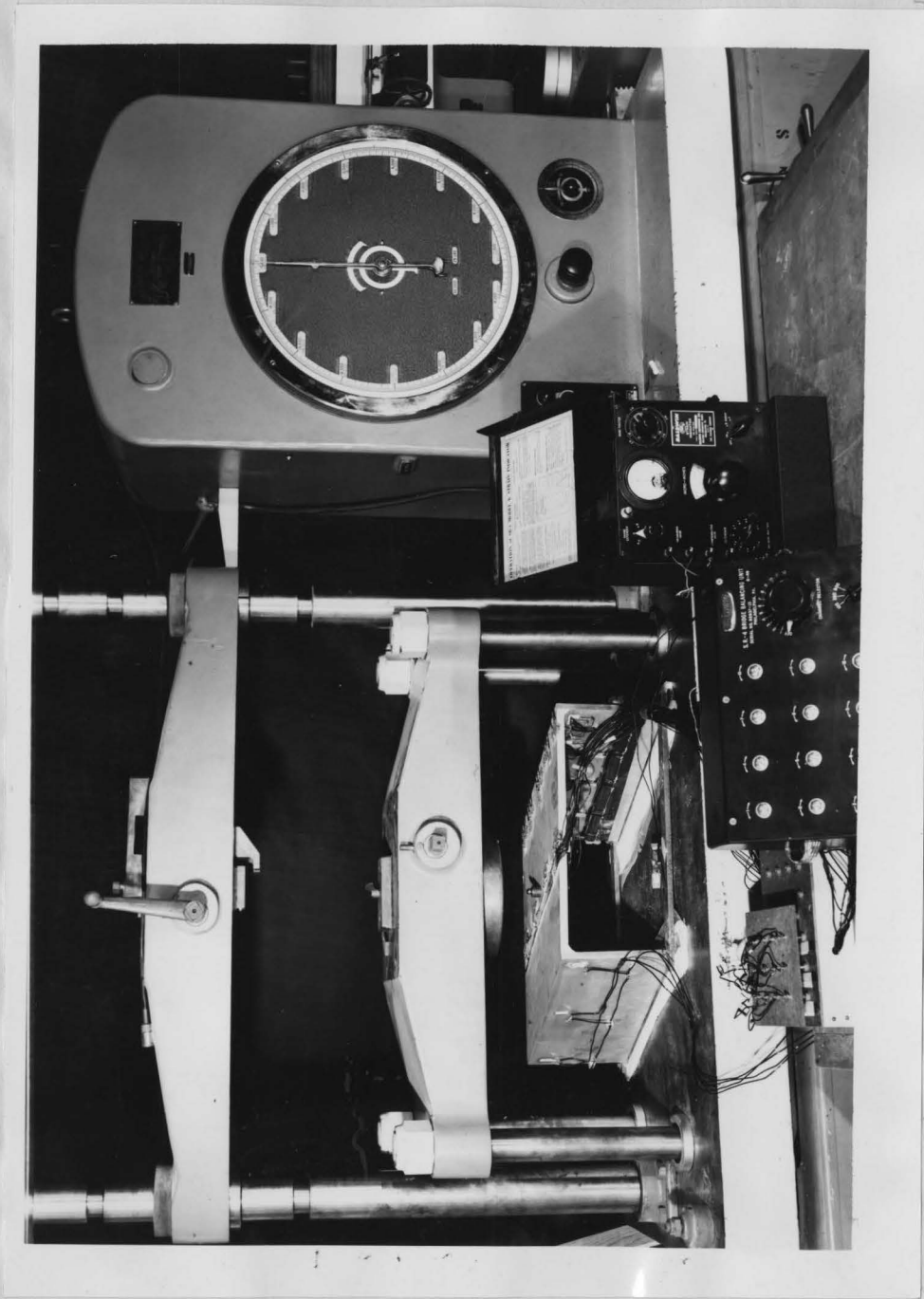


Fig. 8 Concentrated Load Test Apparatus

applied to the model in order that fairly large strains could be obtained. The small surface area made it impractical to obtain the uniform load by the use of weights. It was, therefore, decided to use an elastic contained, filled with air, placed between the head of the testing machine and the deck of the model. The ability of a gas to exert equal pressures in all directions guaranteed that a uniform load over the whole surface of the deck would be obtained.

At first, it was thought that plastic sheeting would prove suitable for construction of the container, but it became impractical when an attempt was made to seal the seam to make it air tight.

A second attempt was made using rubber sheeting; this proved to be very satisfactory. It was necessary to use as thin a rubber sheeting as could be obtained since, the presence of gages and wires on the deck required the sheeting to form around them. The most suitable rubber obtainable had a thickness of $1/32$ of an inch. This was used.

The construction of air tight seams proved to be a relatively simple matter and was accomplished, as illustrated in Figure 7, by the use of ordinary tire patching, purchased in 4 x 12 sheets.



Fig. 9 Uniform Load Test Apparatus

It was decided to construct the bag in rectangular shape since it would make fabrication easier and would provide a loading device for simple type tests.

A valve stem was provided so that air could be pumped into the bag. The valve stem was attached by the hot patch method and the seams were sealed with cold patches, and coated with Goodrich Plio-bond cement.

In order to apply the load to the model, a rectangular box (Figure 7) was constructed of lumber and a section the shape of the deck, but with an approximate clearance of 1 inch all around, cut from the bottom. The inside dimensions of the box were the same as those of the bag. The bag was placed inside the box and inflated.

The box was secured to the head of the testing machine, and the bag inflated until it bulged through the section cut in the box. The unit was brought down until contact was made with the deck, and the amount of air in the bag varied so that all points on the surface of the deck were in contact with the bag under an initial load of 1 psi.

There was some doubt as to the effect compressing the air in the bag would have on its temperature. It was calculated that a rise of 1/2 degree Fahrenheit would cause a strain of six micro-inches. The temperature differential between the

top and bottom surfaces of the deck would cause a bowing of the deck and thus have a deleterious effect on all gages.

To prevent this, the deck was covered with a layer of insulating material.

In order to apply the load to the model, it was necessary to pump air into the bag and measure the load by the reading on the dial of the testing machine. This procedure was necessary to protect the gages since lowering the head of the machine would result in damage to the gages on the outside of the abutment, due to contact with the box. It was also felt that this helped control the effects of changing temperature of the air in the bag.

3. Measurement of Strains.

In order to measure the strains in the 40 SR-4 strain gages located along the knee of the model, it was necessary to use the apparatus illustrated in Figure 9. This arrangement was necessary since the switching and balancing unit could carry a maximum of 12 gages at one time. By incorporating the multi-plug system it was possible to eliminate the laborious task of rewiring the switching and balancing unit after strains of 12 gages were recorded.

As illustrated in Figure 9, 12 wires were permanently connected to the switching and balancing unit from the base of the multi-plug and socket unit. Four multi-plug boards were attached to the active leg of the 40 gages, along the knee, three boards having 12 gages and another board holding the remaining gages. The ground lead was connected directly to the switching and balancing unit from the model.

A compensating gage, consisting of an A-7 strain gage on a piece of the specimens used in testing the properties of the aluminum, was placed directly beneath the bridge and its lead wires connected directly to the switching and balancing unit.

a. Concentrated load test. After the $3/4"$ ϕ steel cylinder was properly located in the panel being tested, the model was loaded to 1575 pounds to settle it in the base, and then the load was removed. This step was followed by loading the model to a load of 75 pounds and zeroing the galvanometer of the Baldwin SR-4, type K strain indicator. This was necessary in order to guarantee that the model was properly seated in the base.

After zeroing the gages, the model was loaded to 1575 pounds and the strains recorded to the nearest five micro-inches per inch for the first 12 gages. The load was then completely removed and the zeroing load of 75 pounds again

applied and the gages checked for zero reading. Errors of more than two micro-inches per inch were considered too large to tolerate and the tests re-run.

The method of using the multi-plug and socket unit proved to be very satisfactory. It was much faster and simpler than rewiring each of the individual gages for each test.

b. Uniform load test. The uniform load test was run before the concentrated load test and the multi-plug and socket unit not used. For this test, the active leads of the gages were wired directly to the switching and balancing unit. The ground for the gages and the compensating gage were wired in the same manner as in the concentrated load test.

Due to the fact that for the uniform load test it was not necessary to move the model once it had been set in its plaster base, under a load of 200 pounds, and since the capacity of the bag was not known, the procedure of applying a large load prior to the zeroing load was not used.

The gages were zeroed at a load of 216 lbs., total load, and the model loaded in increments of 3 psi. to a maximum load of 10 psi. This procedure was necessary since the capacity of the bag was not known and it was felt that if the bag did fail below the desired maximum of 10 psi., the test would not be a

total loss. This fear was unwarranted as the maximum was reached without any trouble.

As mentioned previously, the load was applied by pumping air into the bag by means of an ordinary bicycle pump. There was a slight loss of air at the higher loads, but this was easily controlled with the pump. It is the author's opinion that the loss was due to the fact that the pump was attached at all times and air leaked out of the bag, back through the pump. At no time did the loss of air exceed 0.1 psi., which had no effect on the gage readings when a check was made.

VI. DATA AND RESULTS

As is the usual procedure, the gages were zeroed for a galvanometer reading of 1000 micro-inches per inch and the strains recorded as the indicator read, above or below 1000 micro-inches per inch. Readings below 1000 were compressive and those above were tensile. All readings were taken to the nearest 5 micro-inches per inch.

The strains were converted into stress on the inside and outside faces of the abutment, along section AA in the direction of the Z axis, and on the top and bottom of the deck, along section BB in the direction of the X axis.

The conversion of strain to stress was achieved by use of the stress-strain relationships based on Hooke's law, namely:

$$\epsilon_x = \frac{1}{E} [\sigma_x - (\sigma_y + \sigma_z)]$$

$$\epsilon_y = \frac{1}{E} [\sigma_y - (\sigma_x + \sigma_z)]$$

$$\epsilon_z = \frac{1}{E} [\sigma_z - (\sigma_x + \sigma_y)]$$

Since the σ_z stresses are zero on the outer surfaces, the equations reduce to:

for the deck --- section BB

$$\sigma_x = \frac{E}{1 - \nu^2} (\epsilon_x + \nu \epsilon_y)$$

$$\sigma_y = \frac{E}{1 - \nu^2} (\epsilon_y + \nu \epsilon_x)$$

for the abutment --- section AA

$$\sigma_z = \frac{E}{1 - \nu^2} (\epsilon_z + \nu \epsilon_y)$$

$$\sigma_y = \frac{E}{1 - \nu^2} (\epsilon_y + \nu \epsilon_z)$$

The actual calculation of the stress proceeded as follows:-

The recorded data were converted into the actual strain at the points where the gages were located by subtracting 1000 from the recorded data. The five points a, b, c, d, and e (see detail of model, Figure 2), were selected as the points at which the stress would be computed from the strains. This selection was based on the fact that these points would be the closest to the gages, thus minimizing the distance over which interpolation occurred. Along each section investigated, there were 20 SR-4 strain gages, 10 on each face. The 10 gages on each face were again divided into two groups, those

which measured the strain in the direction of the desired stress and those which measured the strain 90 degrees to the direction of the desired stress.

Since it was impossible to have both gages at a point measure the strains exactly at the point, it was necessary to plot the strains in both directions, on the same paper, at their location along the section and then locate points a to e on this plot and record the values of the strains at these points. An illustration of such a plot may be seen in Figure 10.

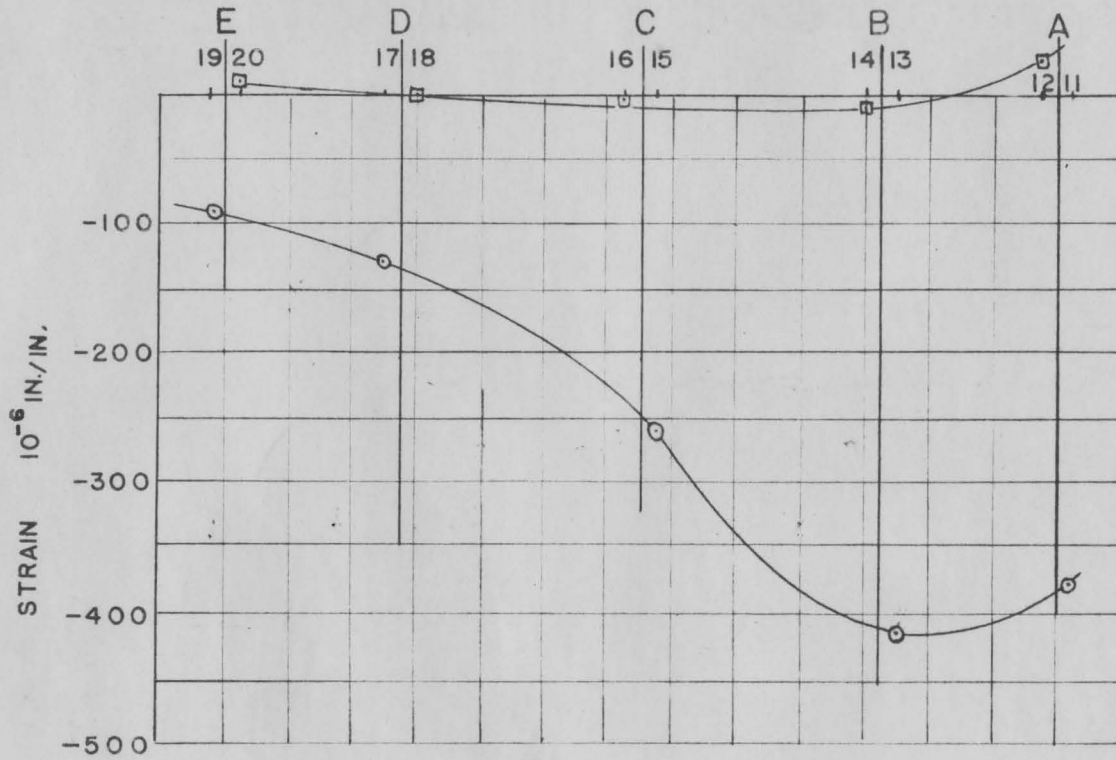
After the strain at the points was recorded, the stress equations were applied and the stress calculated at the five points along the section investigated. In these calculations 0.320 was used for Poisson's ratio, (ν) and 10,360,000 psi. for the Modulus of Elasticity (E).

The stress distribution along section AA of the abutment in the direction of the Z axis, and the stress distribution along section BB of the deck in the direction of the X axis are shown in Figures 11 through 30.

PANEL O

SECTION AA

GAGES	ϵ_x INSIDE OF ABUTMENT					ϵ_y INSIDE OF ABUTMENT				
	11	13	15	17	19	12	14	16	18	20
STRAIN $\times 10^6$	-380	-415	-260	-130	-90	+30	-10	-5	0	+10



σ_z & σ_y INSIDE OF ABUTMENT

POINT	ϵ_z	ϵ_y	$\epsilon_z + \nu \epsilon_y$	$\epsilon_y + \nu \epsilon_z$	σ_z	σ_y
A	-393	+34	-382	-92	-4390	-1060
B	-410	-9	-413	-140	-4755	-1610
C	-251	-7	-253	-87	-2910	-1000
D	-136	0	-136	-44	-1565	-500
E	-94	+10	-91	-20	-1045	-230

FIG.10 SAMPLE CALCULATION

STRESS DISTRIBUTION

UNIFORM LOAD SECTION AA

9 LBS. PER SQ. IN.

OUTSIDE ○ ○
INSIDE ● ●

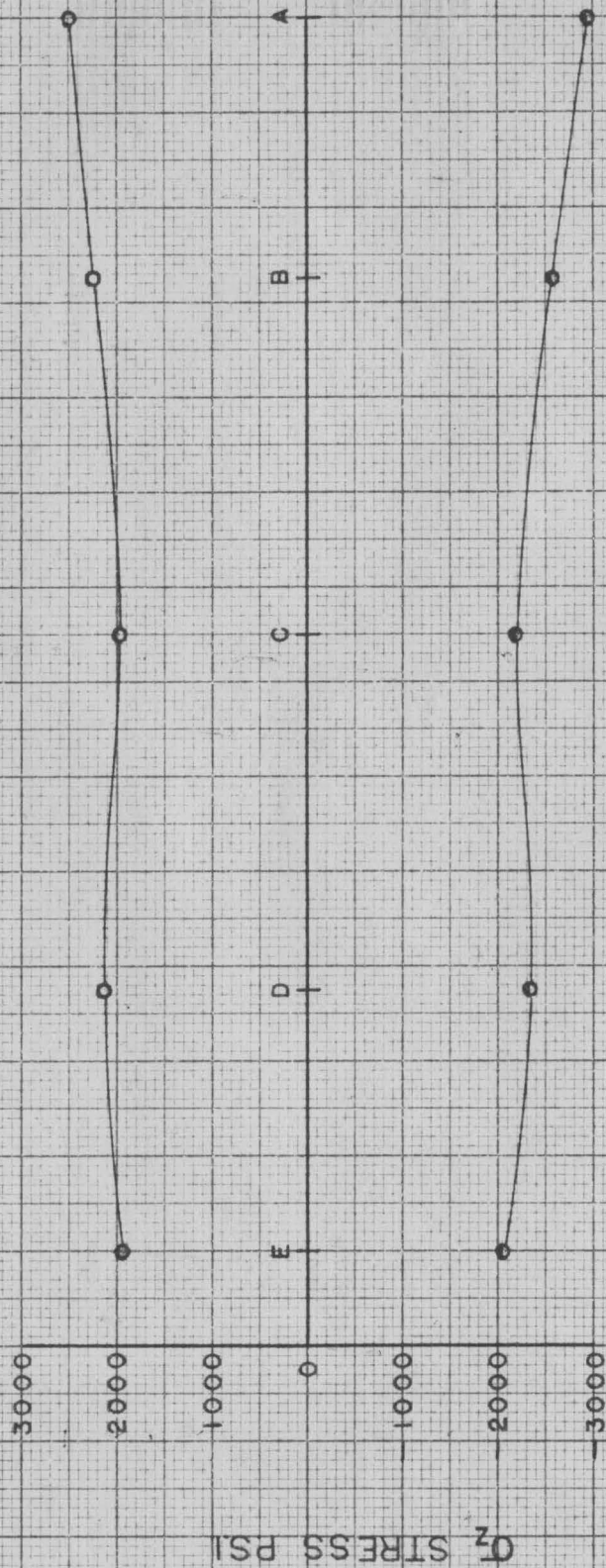


FIG. II

STRESS DISTRIBUTION

UNIFORM LOAD SECTION BB

9 LBS. PER SQ. IN.

TOP  — 

BOTTOM  — 

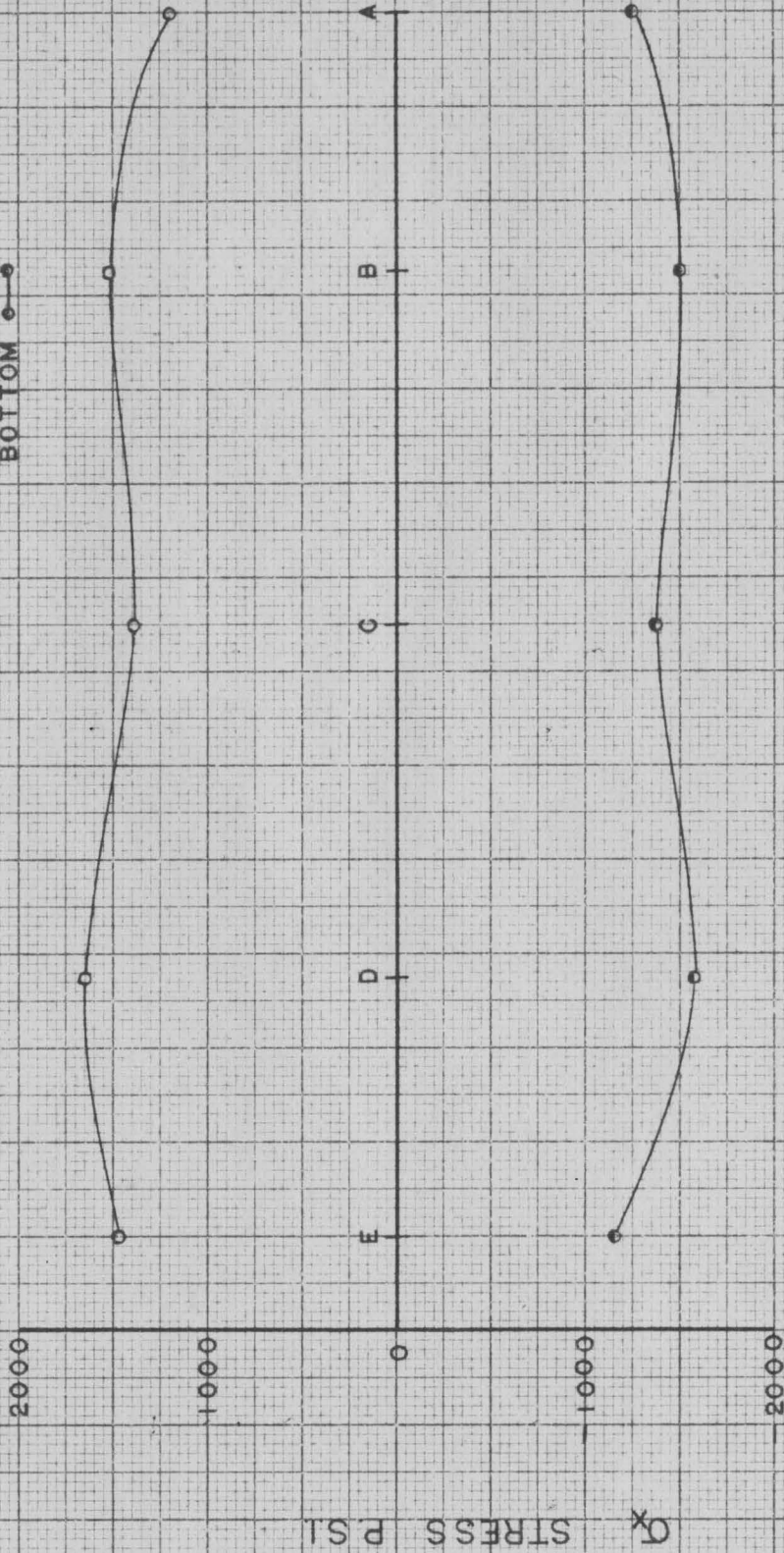


FIG12

STRESS DISTRIBUTION PANEL O SECTION AA

1500 LB LOAD
OUTSIDE —○—
INSIDE —○—

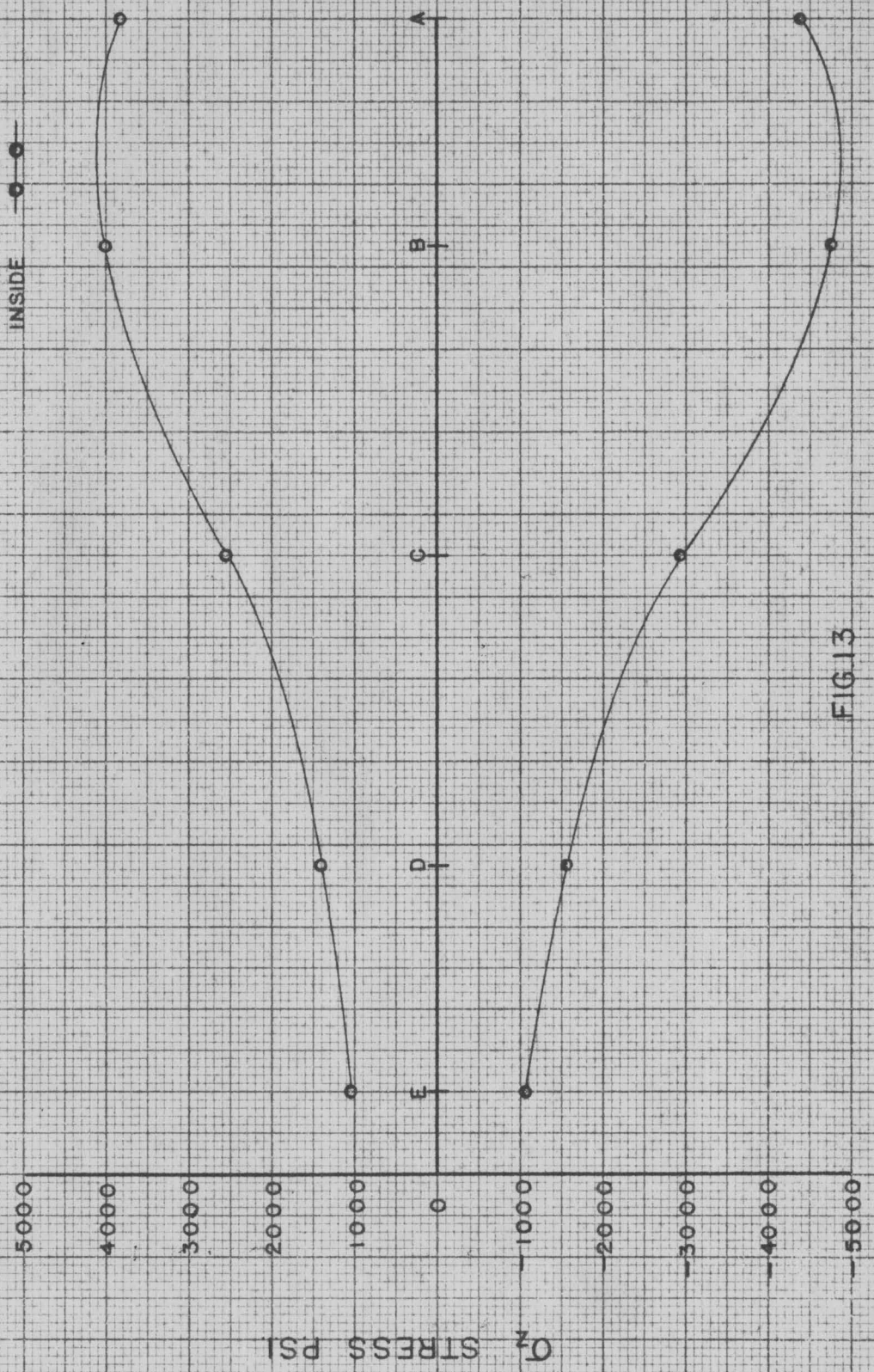


FIG. 13

STRESS DISTRIBUTION

PANEL O SECTION BB

1500 LB. LOAD

TOP
BOTTOM

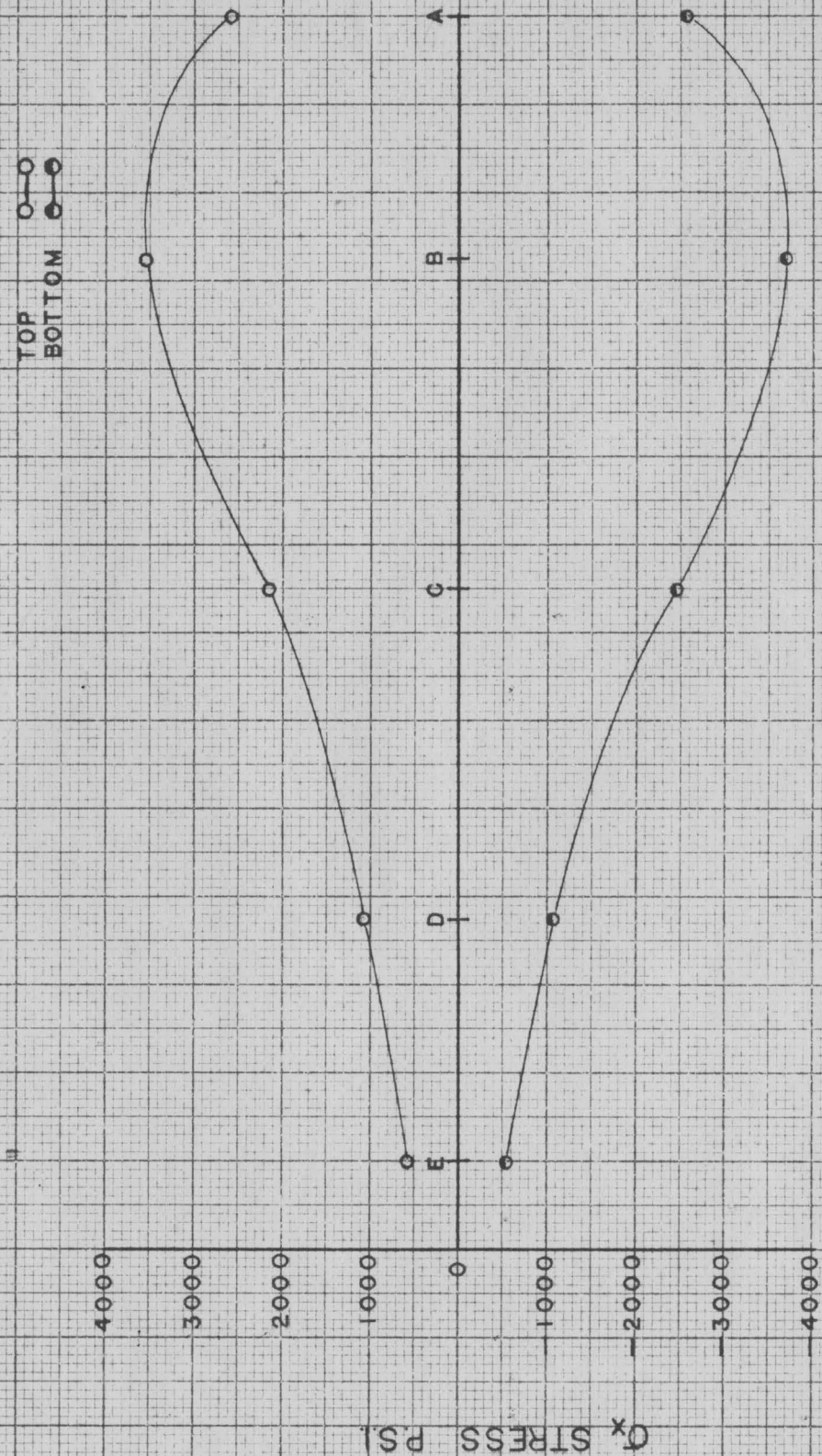


FIG. 14

STRESS DISTRIBUTION

PANEL I SECTION A A

1500 LB. LOAD

OUTSIDE
INSIDE

Q_z STRESS PSI

4000
3000
2000
1000
0
-1000
-2000
-3000
-4000
-5000
-6000

A
B
C
D
E

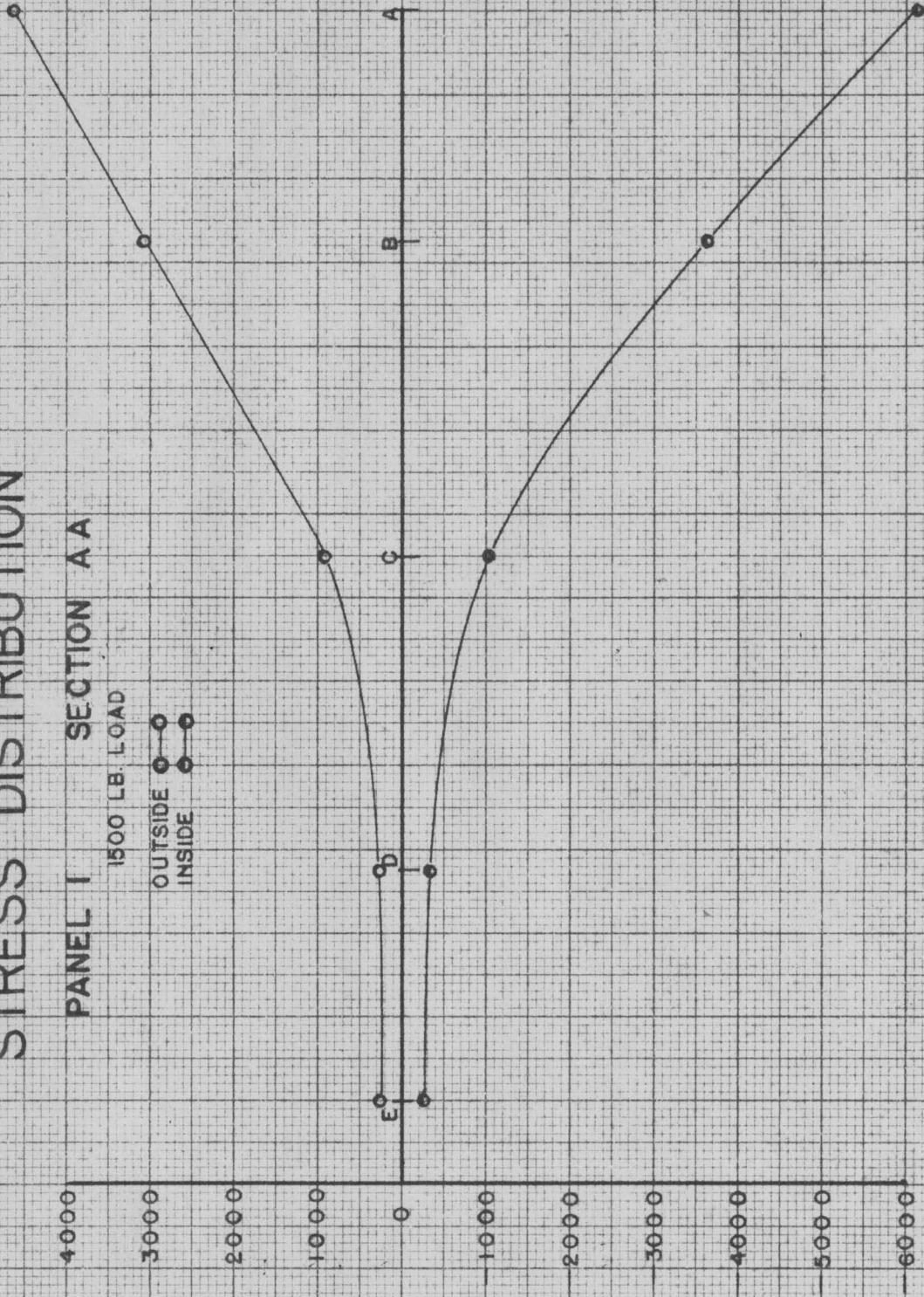


FIG 15

STRESS DISTRIBUTION

PANEL I SECTION BB

1500 LB. LOAD

TOP ○—○
BOTTOM ●—●

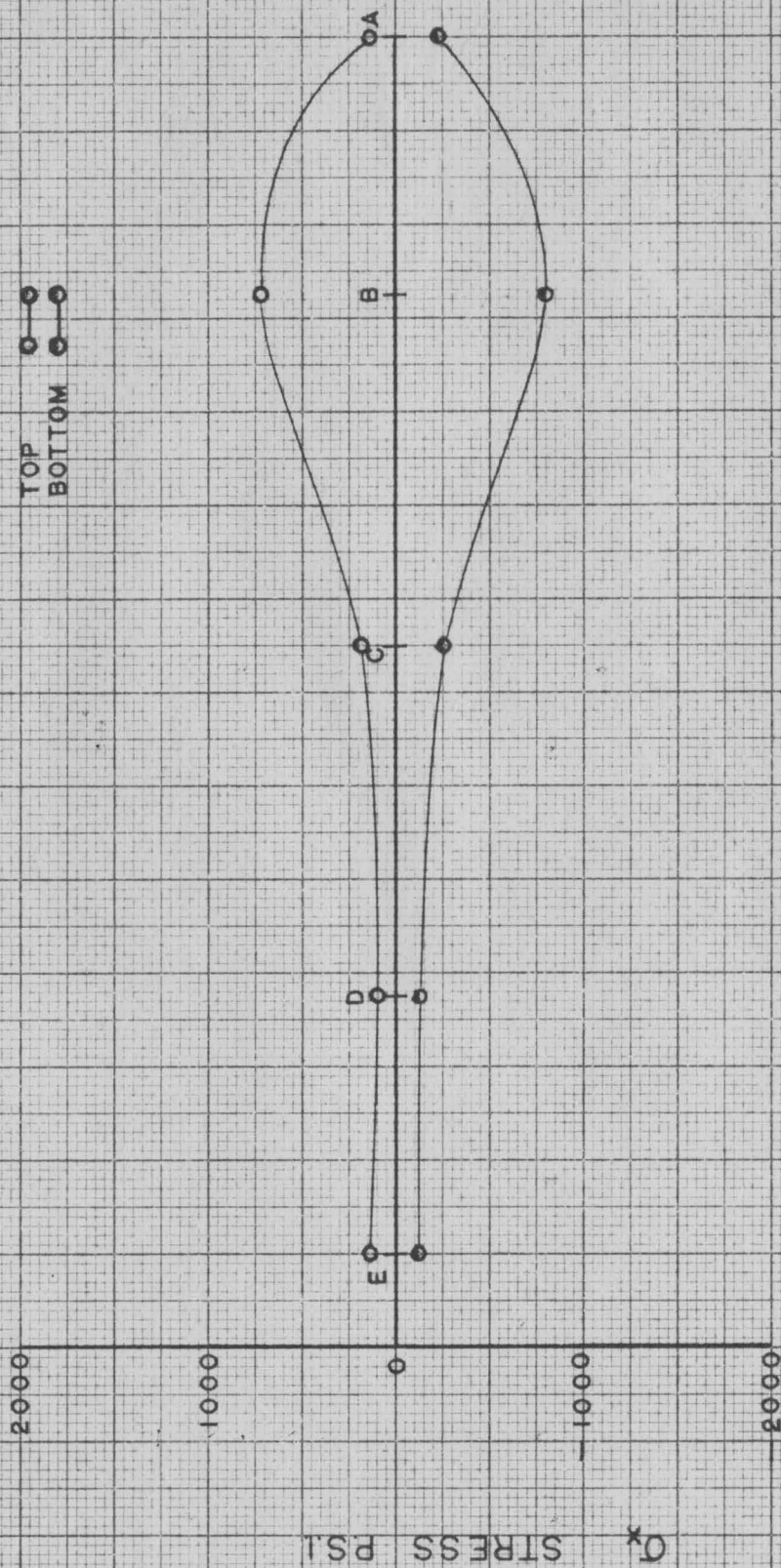


FIG. 16



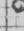
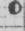
Qx STRESS PSI

2000
1000
0
1000
2000

STRESS DISTRIBUTION

PANEL II SECTION AA

1500 LB. LOAD

OUTSIDE  
INSIDE  

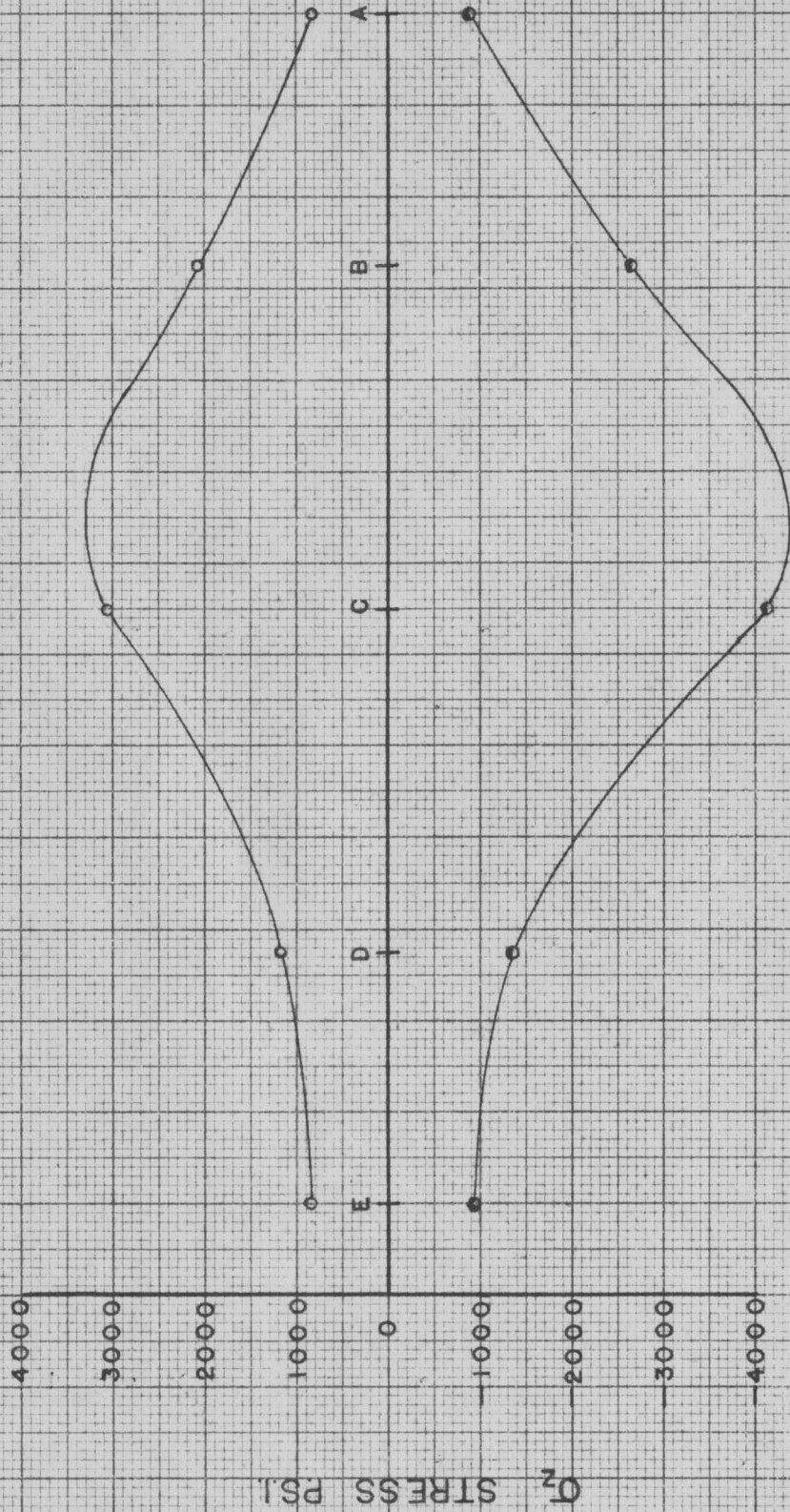




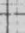

FIG. 17

Engraving 7 X 10 in.
MADE IN U.S.A.

STRESS DISTRIBUTION

PANEL II SECTION BB

1500 LB. LOAD

TOP  
BOTTOM  

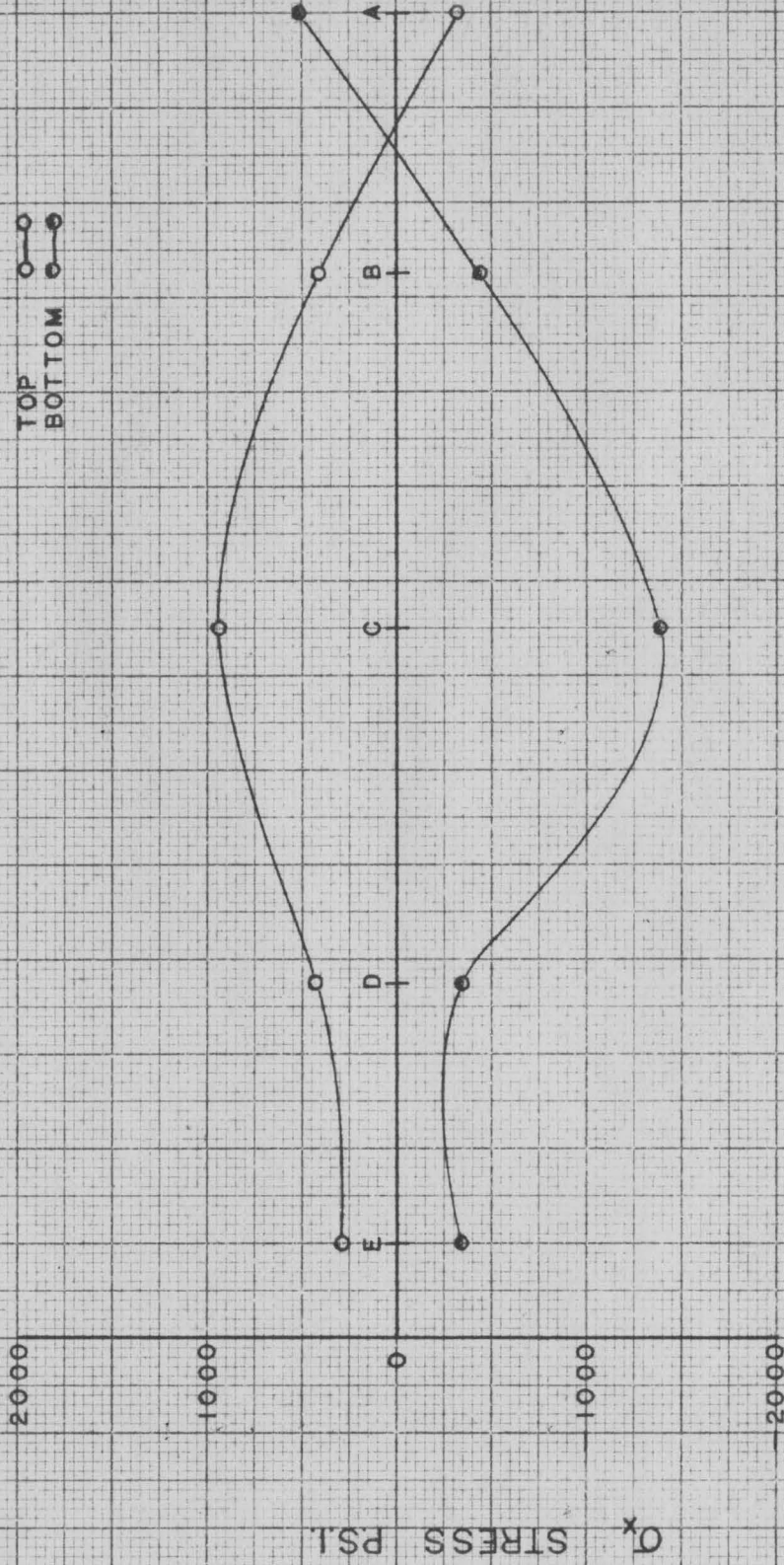


FIG.18

STRESS DISTRIBUTION

PANEL III SECTION AA

1500 LB. LOAD

OUTSIDE ○ ○
INSIDE ● ●

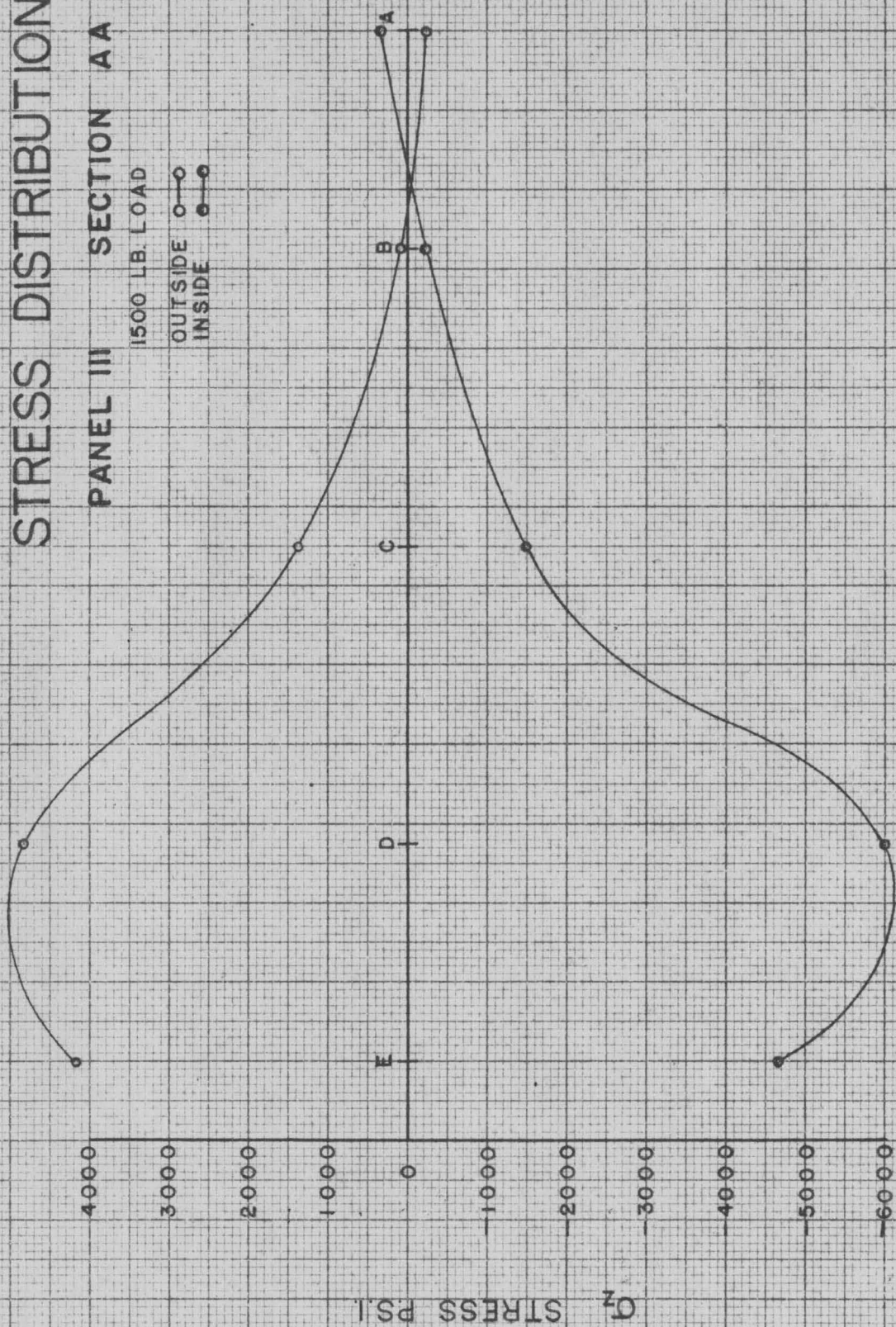





FIG. 19

σ_z STRESS PS.I.

STRESS DISTRIBUTION

PANEL III SECTION BB

1500 LB. LOAD

TOP  
BOTTOM  

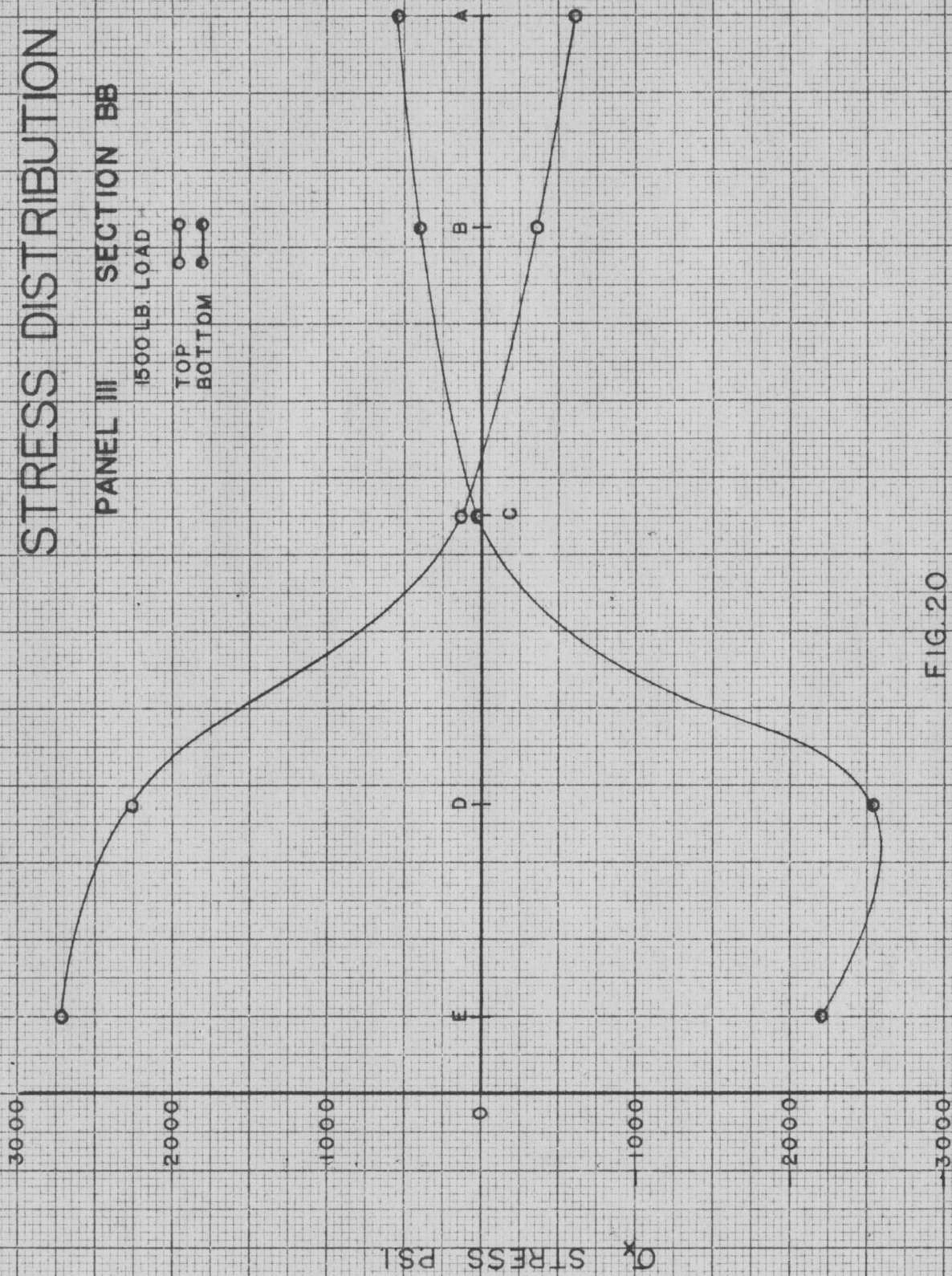


FIG. 20

STRESS DISTRIBUTION

PANEL IV SECTION AA

1500 LB. LOAD

OUTSIDE ○—○
INSIDE ●—●

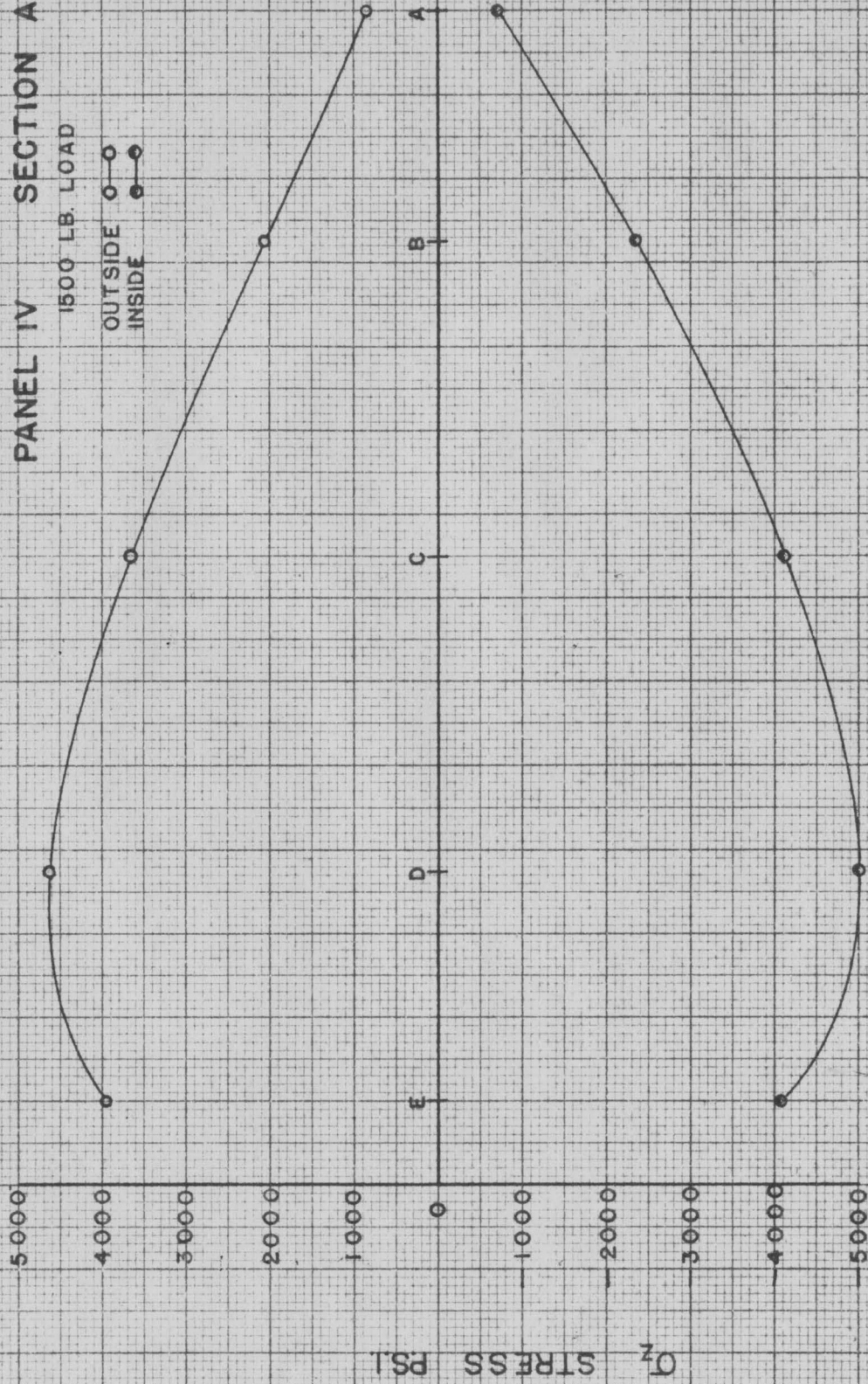


FIG 21

STRESS DISTRIBUTION

PANEL IV SECTION BB

1500 LB LOAD

TOP  
BOTTOM  

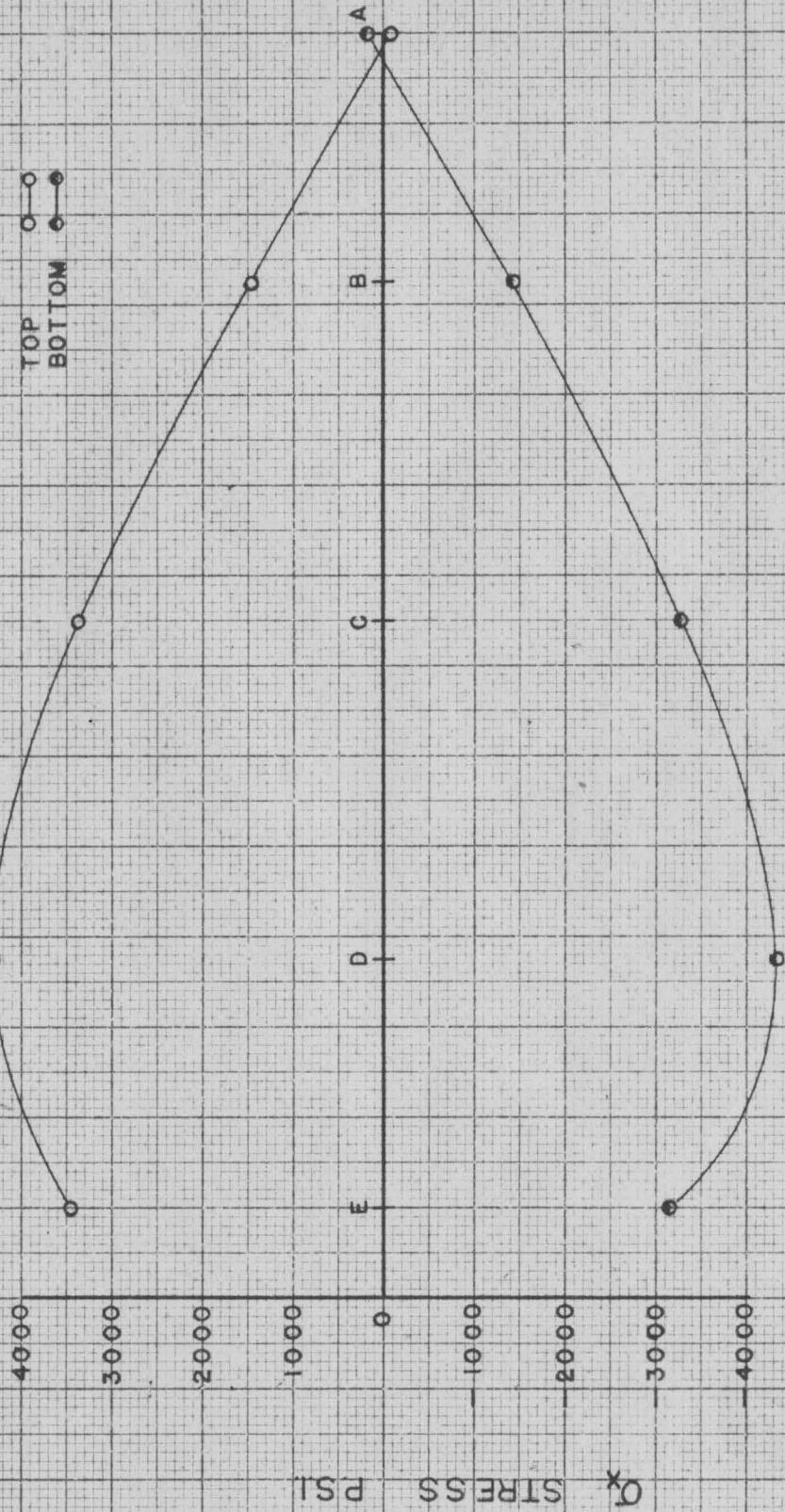


FIG. 22

STRESS DISTRIBUTION

PANEL V SECTION AA

1500 LB. LOAD

OUTSIDE ○—○
INSIDE ●—●

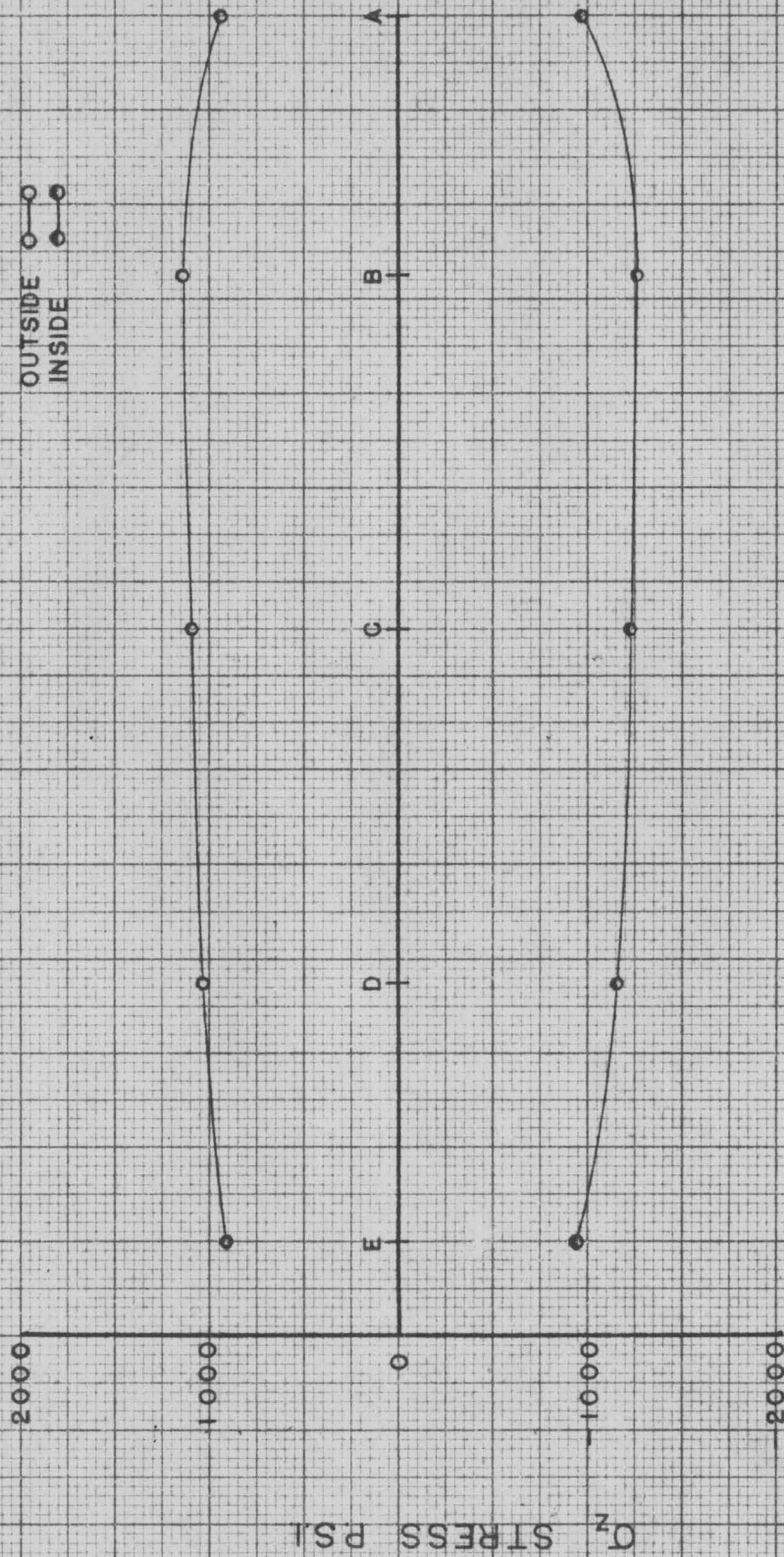






FIG. 23

STRESS DISTRIBUTION

PANEL V SECTION BB

1500 LB. LOAD

TOP  
BOTTOM  

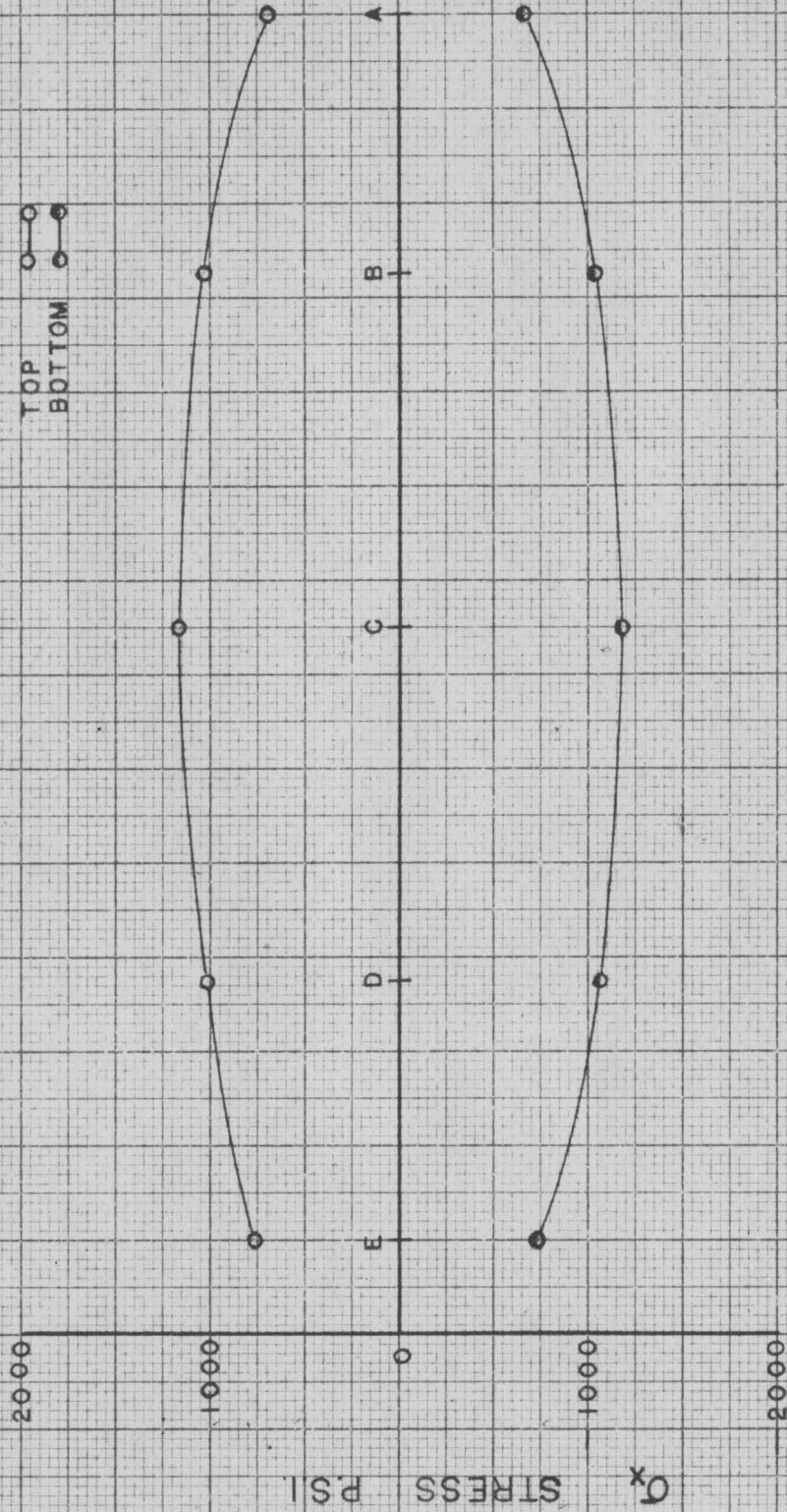


FIG. 24

STRESS DISTRIBUTION

PANEL VI SECTION AA

1500 LB. LOAD
OUTSIDE
INSIDE

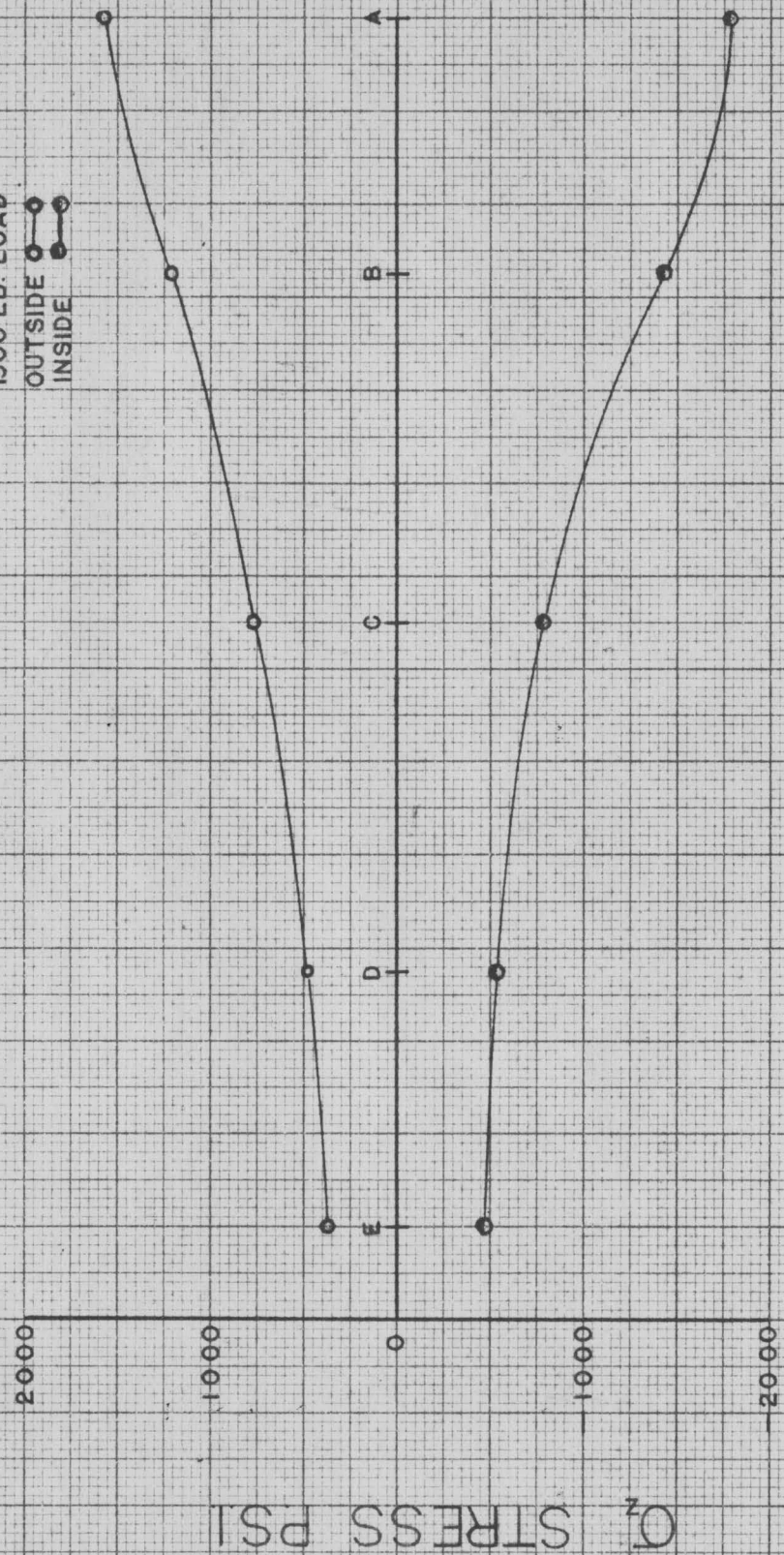


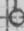



FIG. 25

STRESS DISTRIBUTION

PANEL VI SECTION BB

1500 LB. LOAD

TOP  
BOTTOM  

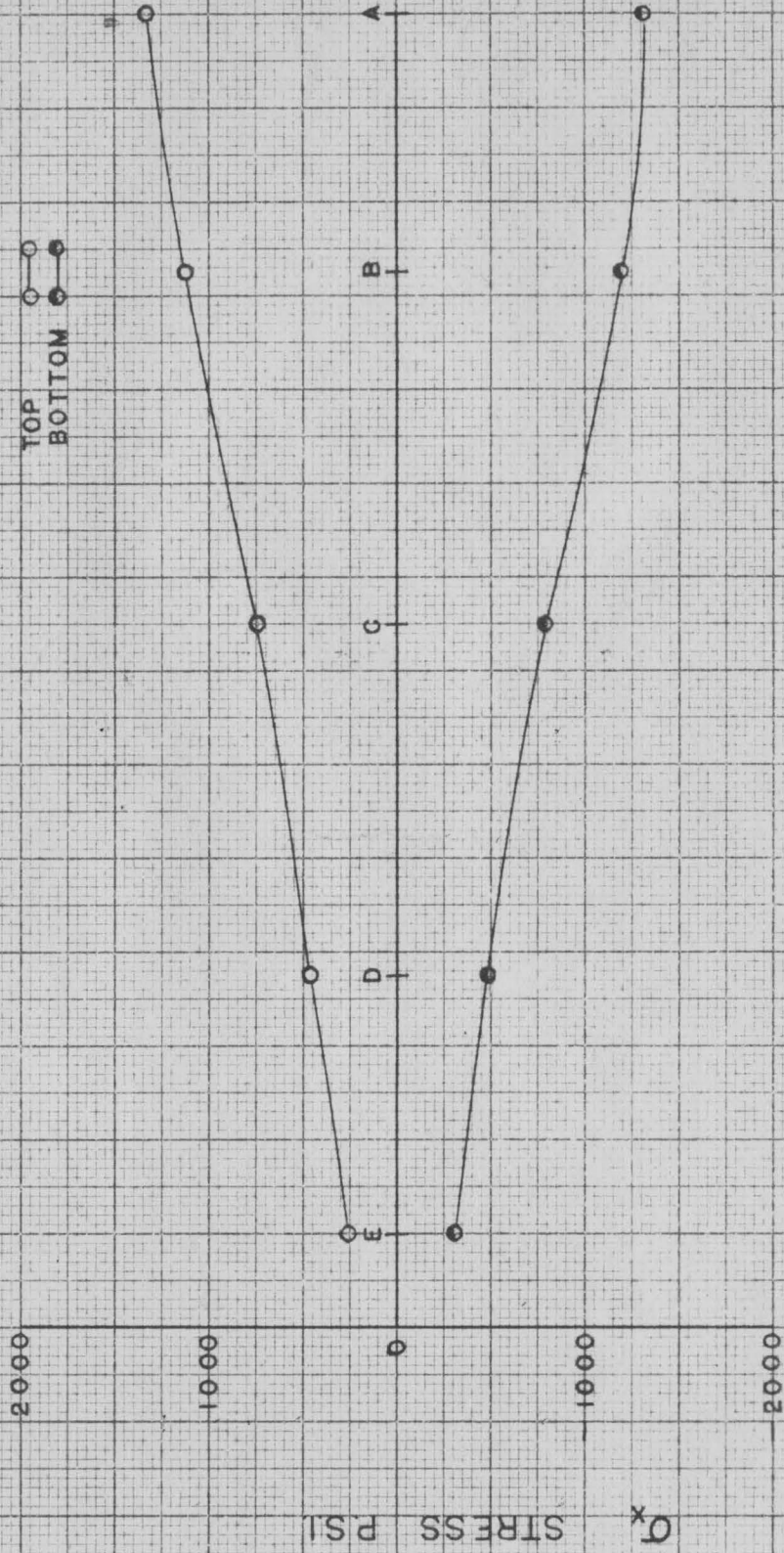


FIG. 26

STRESS DISTRIBUTION

PANEL VII SECTION AA

1500 LB. LOAD

OUTSIDE

INSIDE

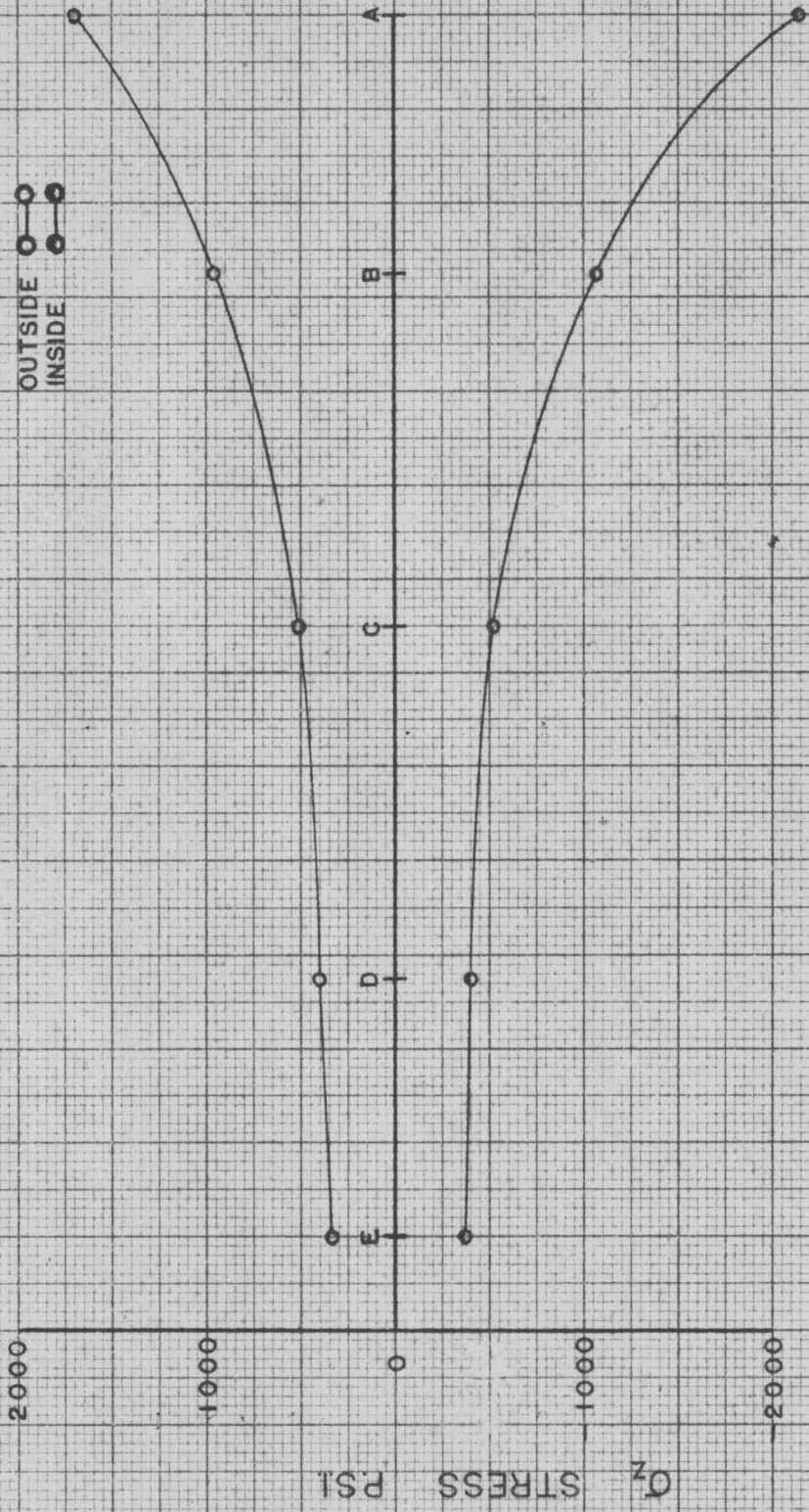


FIG. 27

STRESS DISTRIBUTION

PANEL VII SECTION BB

1500 LB. LOAD

TOP ○
BOTTOM ●

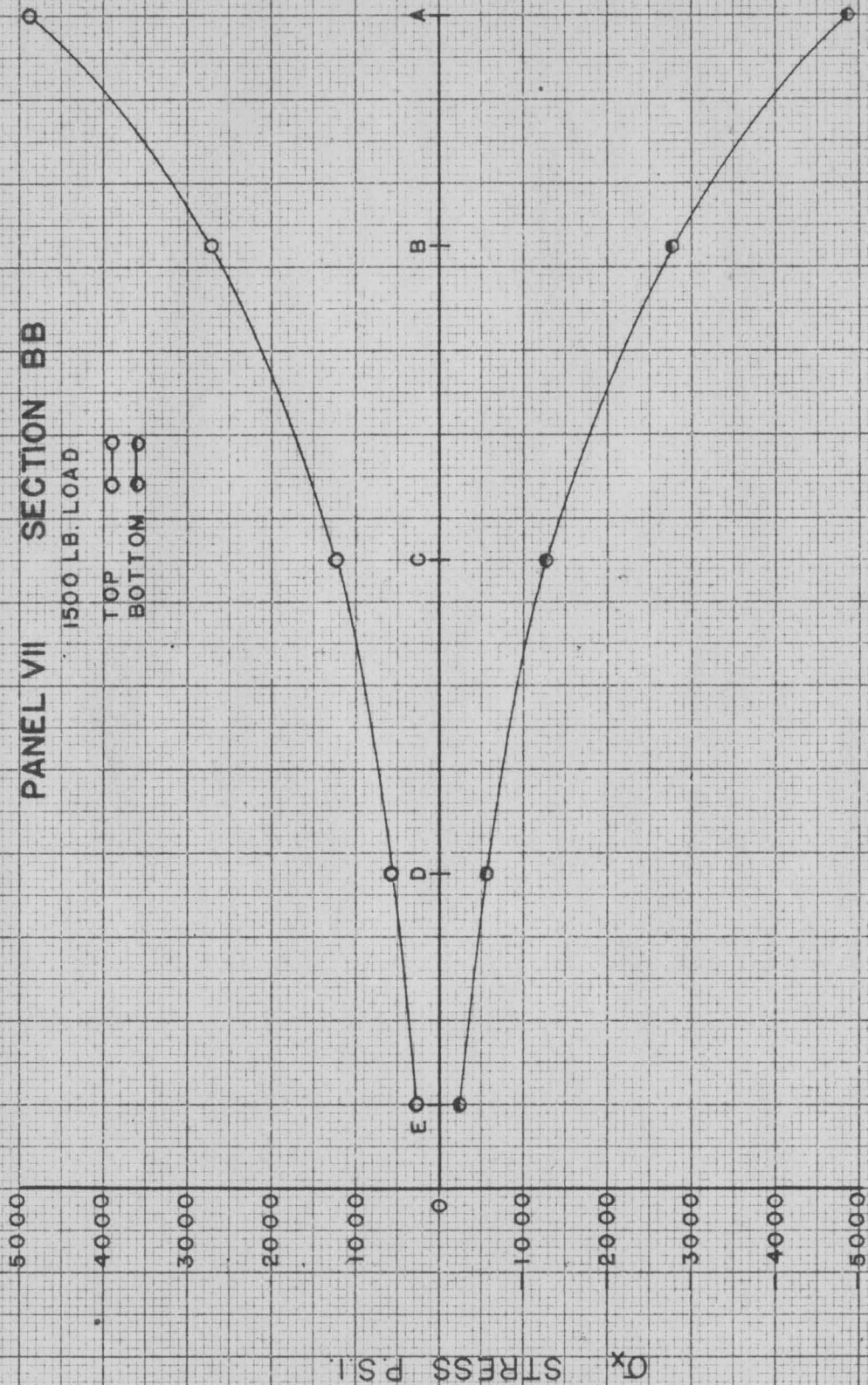


FIG. 28

Ox STRESS P.S.I.

STRESS DISTRIBUTION

PANEL VIII SECTION AA

1500 LB. LOAD

OUTSIDE ○—○
INSIDE ○—○

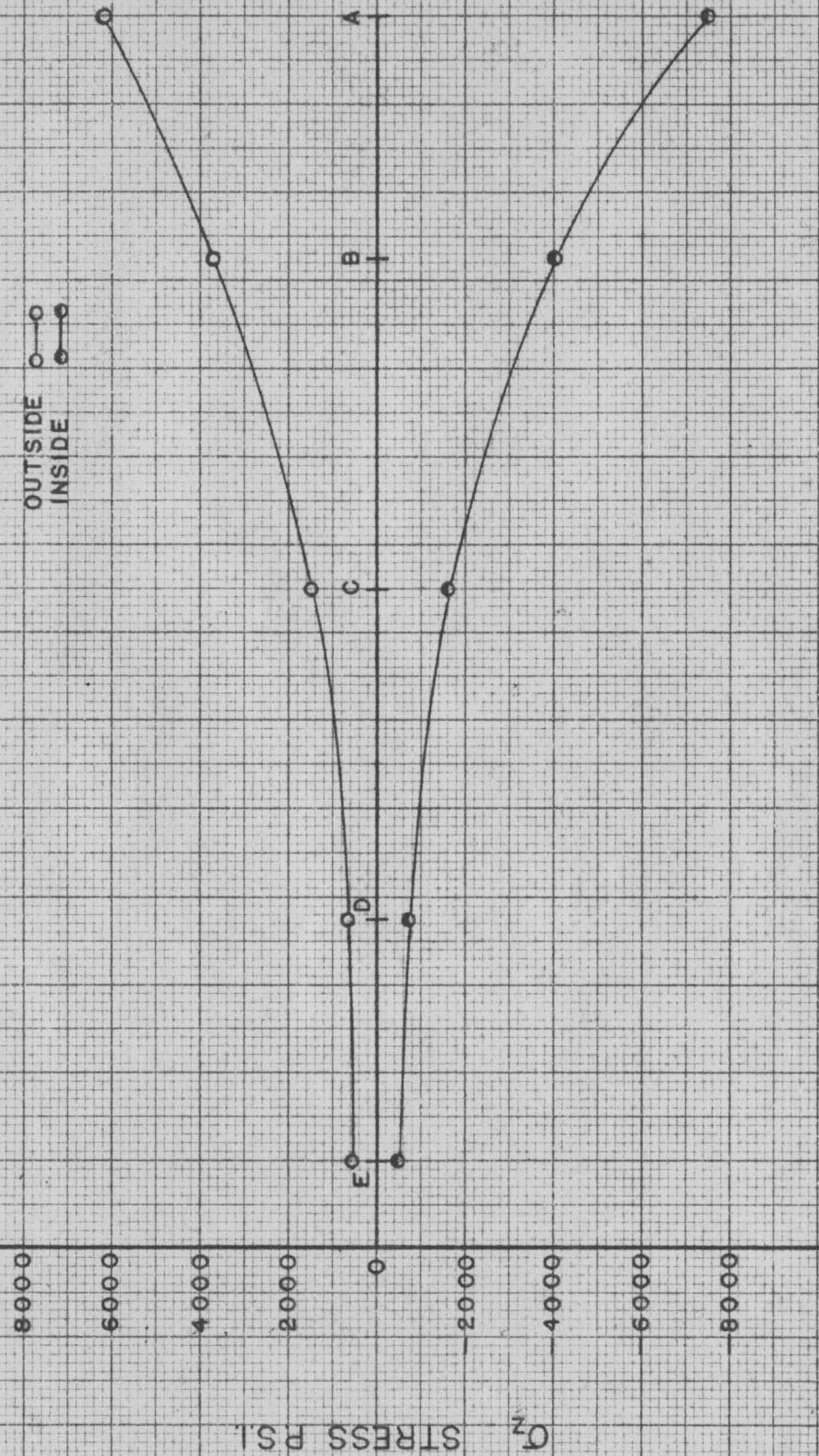


FIG. 29

STRESS DISTRIBUTION

PANEL VIII SECTION BB

1500 LB. LOAD

TOP ○—○
BOTTOM ●—●

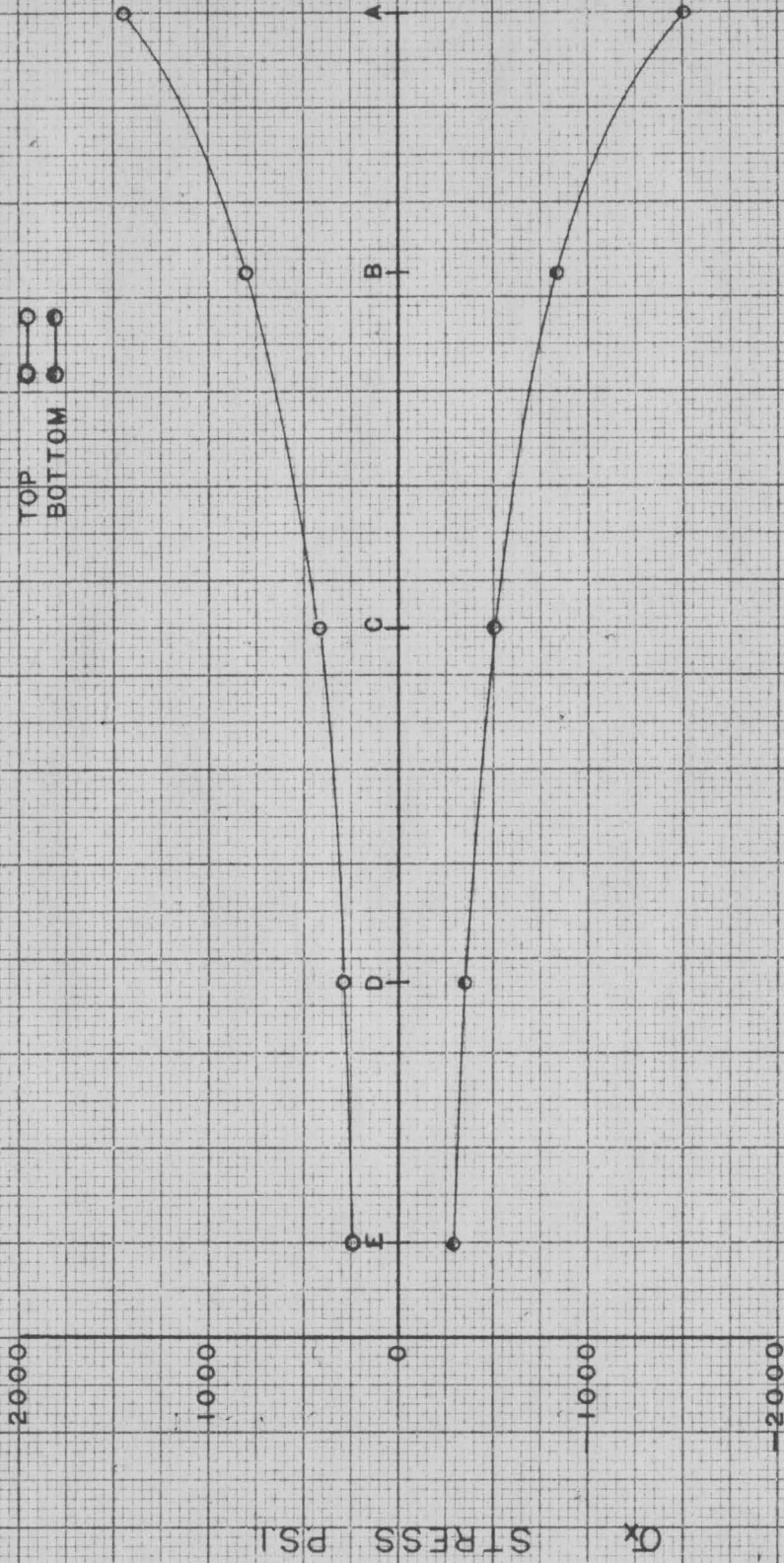


FIG. 30

VII. DISCUSSION

A. Curves

The curves of stress distribution presented in this thesis are, in the author's opinion, a good representation of the stress distribution along the knee of the model for the various loading conditions considered. There may be some doubt in the reader's mind as to the location of the maximum point of a particular curve. This is justifiable. The shape of the curves is to some degree the result of the author's imagination and intuition. Due to the lack of a greater number of data points it was not possible to determine accurately the true shape of the curve. This difficulty is especially noticeable on the curves where the maximum data points occur at points a or e, the points nearest the end of the sections. Since there was no reason to justify any assumption as to the magnitude of the stress along the free edges of the model, it was not possible to tell whether the maximum occurred before the last data point on the curve, between the last data point and the edge of the model, or at the edge of the model. It is for this reason that the curves were discontinued at the last data point.

The above discussion does not dispute in any way the validity of the results of the investigation; it merely points out the possibility that the shape of the curves may not be true in some regions, particularly those mentioned above. The author believes that the data points are accurate within the limits of the experimental observation and, consequently, the general trend of the curves is accurate. As mentioned in Section V 3.a. of this thesis, all zero readings were checked after completion of a test run. If a difference of more than 2 micro-inches per inch was found, the test was re-run. As another check on the experimental results, an arbitrary group of gages were selected, after the experimental investigation was completed, and an attempt was made to reproduce the strain readings previously recorded for these gages. The results were very gratifying; of the 12 gages checked only three were in error, all by 5 micro-inches per inch. It is also significant to mention that the smallest strain measured by these three gages was 215 micro-inches per inch, which is an error of only 2.3 per cent. It was believed that since this group of gages checked with the above mentioned accuracy and since all zero readings were checked, that it was not necessary to recheck all gages for all loadings.

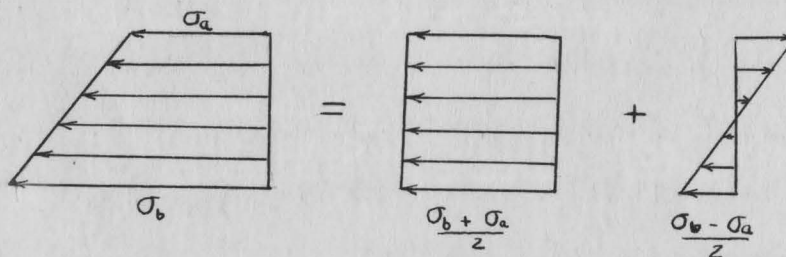
A check on the uniform load investigation was also made by the same method described above. The maximum error encountered was 5 per cent.

The author believes that the above mentioned checks are evidence of the validity of the data points and the general trend of the curves.

B. Interpretation of Curves

The curves of stress distribution, Figures 11 through 31, can be used to determine the normal stress and bending stress distribution along sections AA and BB if certain assumptions are made.

In an attempt to check the accuracy of the experimental results, the author used the following assumptions and equations to calculate the normal stress along the abutments at the data points (a, b, c, d, and e).



Linear Stress Distribution

Figure 31

A linear distribution of stress is assumed throughout the plate, see Figure 31, and it may be concluded that the following is true.

For section AA - abutment

$$\text{Normal Stress} = \frac{\sigma_z)_i + \sigma_z)_o}{2}$$

$$\text{Bending Stress} = \frac{\sigma_z)_i - \sigma_z)_o}{2}$$

For section BB - deck

$$\text{Normal Stress} = \frac{\sigma_x)_b + \sigma_x)_t}{2}$$

$$\text{Bending Stress} = \frac{\sigma_x)_b - \sigma_x)_t}{2}$$

With the value of the normal stress, at the data points, a normal stress distribution curve was plotted. The area under the curve was measured with a planimeter three times and the average area calculated. The total normal thrust on the abutment was then computed by multiplying the area under the curve by the proper scale factors and the thickness of the plate.

The assumption was then made that, due to the symmetry of the model, the panel loadings could be combined to calculate the total thrust in both abutments. More explicitly, the

thrust for a load in Panel I in one abutment would be the same as the thrust in the other abutment due to a load in Panel V.

Employing the above assumptions and computations, the author made a static check on the results by comparing the total thrust on the abutments, ΣV , and the applied load of 1500 pounds. The per cent difference for the various panels are tabulated in Table 2.

$$\text{per cent difference} = \frac{\Sigma V - 1500}{1500}$$

Table 2

<u>Panel</u>	<u>Per Cent Difference</u>
O	80
I	26.7
II	47.8
III	26.7
IV	57.5
Uniform load	7

The variation in the applied load and thrust in the abutments is probably due to factors inherent in the model, to errors in the assumptions, and to the fact that the thrust is

obtained by taking the difference of two large numbers, both of which may be very accurate.

The assumptions of a linear stress distribution throughout the thickness of the plate may not be perfectly true. It was not possible to check this assumption.

The possibility of an error being introduced in the assumption of symmetry also exists. An attempt was made to check this assumption by attaching strain gages on the outside face of the abutment, not investigated previously, at points symmetrically opposite a, c, and d. Although the check was not exhausting, due to the use of only three gages, it did indicate that some error might exist in the assumption of symmetry. Comparing the strains measured by the three check gages with the strain observed previously, under the same loading conditions, at the three symmetrically opposite points, the variation exceeded 10 per cent in only two cases. In both cases, the strain was less than 100 micro-inches per inch. On this basis the author believes that any error due to dissymmetry would not exceed 10 per cent.

A factor which the author believes might account for the variation between the applied load and the total-thrust, in the abutments, is the existence of a stress concentration factor due to the fillet weld. In all the variations

encountered, the total vertical thrust was always greater than the applied load. Since the strains on the inside faces were measured as close to the toe of the fillet as was possible, it is quite possible that localized effects of the fillet influenced the gage readings.

Based on the above considerations and attributing all the discrepancy to the fillet, the author calculated the average stress concentrations factors shown in Table 3, by the following formula:

$$t \int \frac{K \sigma_z)_i + \sigma_z)_o}{2} dx + t \int \frac{K \sigma_z)_i' + \sigma_z)_o'}{2} dx = W$$

Table 3

Panel	K
0	1.100
I	1.040
II	1.071
III	1.060
IV	1.064
Uniform load	1.017

It must be remembered that the values of K in Table 3 are an average for the abutment.

The distribution of normal stress along Section BB of the deck consisted of both tensile and compressive stresses. This was probably due to a warping of the deck by the abutments lifting at one of their corners. Deflection measurements taken near the corners of the deck with an Ames dial reading to the nearest ten-thousands of an inch are recorded in Figure 32. The possibility that the deck did warp is evident from Figure 32.

The purpose of this discussion was to present a method of calculating normal stress and bending stress along Sections AA and BB and to present possible factors which might have affected the strain reading. It does not affect the stress distribution curves presented in this thesis since they represent the distribution of stress as it occurred in the model.

C. Sideway

Sideway was probably eliminated in the concentrated load test due to the method of loading. The friction between the $3/4"$ ϕ loading block and the surface of the model was probably sufficient to prevent movement of the model. The same cannot be assumed in the case of the uniform load test since the method of loading did not offer any restraint to movement of the model.

DEFLECTIONS AT THE CORNERS OF THE DECK

1500 LB. LOAD

10^{-4} INCHES

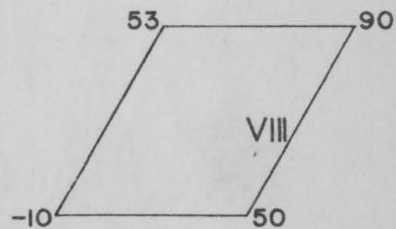
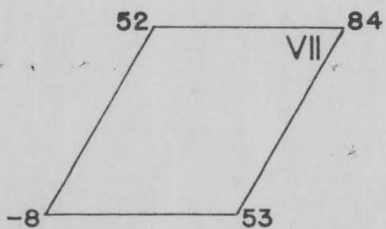
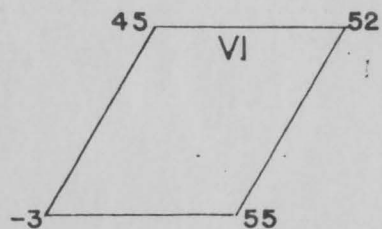
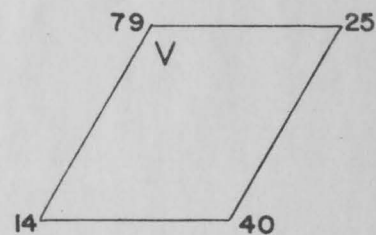
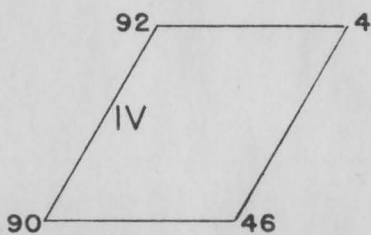
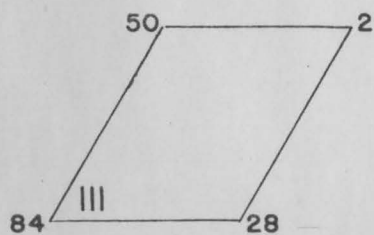
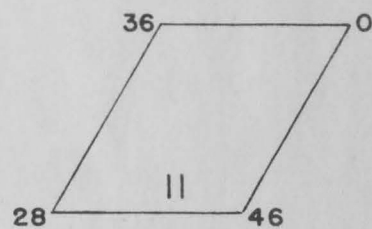
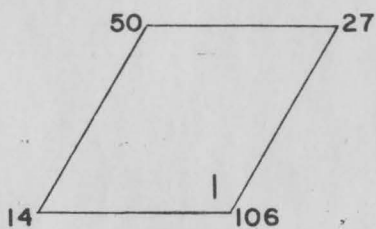
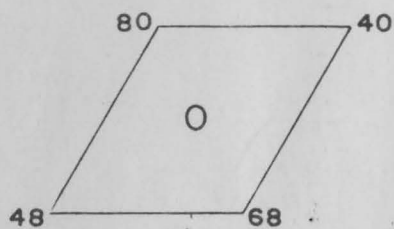
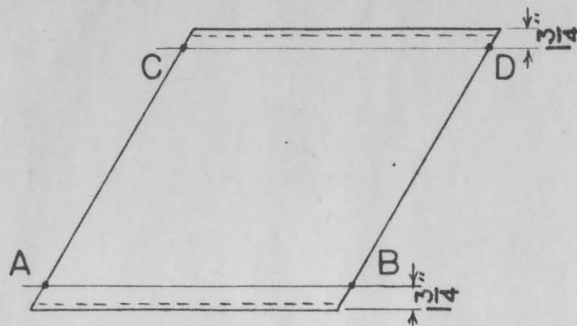


FIG. 32

VIII. CONCLUSIONS

The results of this investigation were not compared with any theories now in use for skewed rigid frames. It is, therefore, not possible to make any conclusions as to the validity of these theories.

The results of the investigation do indicate that:

1. The point of maximum stress lies near to a line drawn through the point of loading and perpendicular to the abutment.

2. Welded aluminum models may be used satisfactorily for investigations involving rigid frame bridges.

IX. RECOMMENDATIONS

The author wishes to make the following recommendations for future work of this type.

1. In order that the trend of the stress distribution curves may be determined more accurately, a greater number of gages should be incorporated, particularly at the end portions of the sections investigated.

2. Consideration be given to fillet and it's effect on the strains.

3. An attempt should be made to determine a stress concentration factor for the fillet.

4. A correction for dissymmetry should be undertaken by investigating the other abutment of the model for the various loading conditions.

X. ACKNOWLEDGMENTS

The author is deeply indebted to Prof. Dan Frederick for his very able and willing assistance in overcoming the problems encountered in this investigation. The author also wishes to express his gratitude to Prof. D. H. Pletta for giving him the opportunity to undertake this investigation, and for his advice on the problems encountered.

XI. BIBLIOGRAPHY

- ✓1. Barron, M., Reinforced Concrete Skewed Rigid-Frame and Arch Bridges, Proceedings of the American Society of Civil Engineers, Vol. 76, Separate 13, April, 1950.
- ✓2. Fisher, G. P. and Boyer, W. G., Reactions of a Two-Span, Skewed, Rigid Frame Bridge, Highway Research Board, Research Report 14-B, p. 75.
3. Gifford, E. F., Approximate Design Method for Concrete Rigid Frames, Engineering News-Record, May 3, 1934, p. 547.
- ✓4. Hayden, A. G., The Rigid Frame Bridge, John Wiley and Sons, Inc., 1931.
- ✓5. Hodges, R. M., Simplified Analysis of Skewed Reinforced Concrete Frames and Arches, Transactions of the American Society of Civil Engineers, Vol. 109, (1944), p. 913.
- ✓6. Michalos, J. P., Analysis of Skewed Rigid Frames and Arches, Journal of the American Concrete Institute, February, 1952, p. 437.
- ✓7. Rathbun, J. C., Analysis of Stress in the Ring of a Skewed Arch, Transactions of the American Society of Civil Engineers, Vol. 87, (1924), p. 611.

- ✓8. Rathbun, J. C., An Analysis of Multiple-Skew Arches on Elastic Piers, Transactions of the American Society of Civil Engineers, Vol. 98, (1933), pp. 11-14.
- ✓9. Weiner, B. L., Design of a Reinforced Concrete Skew Arch, Transactions of the American Society of Civil Engineers, Vol. 96, (1932), p. 1212.
- ✓10. Weiner, B. L., Practical Design of Solid-Barrel, Reinforced Concrete Skew Structures, Proceedings of the American Society of Civil Engineers, Vol. 76, Separate 39, October, 1950.
- ✓11. Weiner, B. L., (Discussion) An Analysis of Multiple-Skew Arches on Elastic Piers, by J. C. Rathbun, Transactions of the American Society of Civil Engineers, Vol. 98, (1933), pp. 46-55.
12. Unusual Bridge Test Involves Rigid Frame Built on Skew, Southwest Builder and Contractor, August 21, 1936. (Reprinted by Portland Cement Association).
- ✓13. Unusual Concrete Rigid-Frame Test, Engineering News-Record, November 17, 1938, pp. 615-617.
- ✓14. Smith, L. T. and Lillard, P., Extensometer Stress Measurements, North Avenue Bridge, Chicago, Ill., Transactions of the American Society of Civil Engineers, Vol. 107, (1942), pp. 1447-1469.

**The vita has been removed from
the scanned document**